AN INVESTIGATION OF POLYMER ENCAPSUALTED GOLD NANOPARTICLES FOR USE IN ANALYTICAL METHODS FOR PROTEOMIC BASED RESEARCH

A Thesis

by

PHILLIP LANG

Submitted to the Office of Graduate and Professional Studies of
Texas A&M University
in partial fulfillment of the requirements for the degree of

MASTER OF SCIENCE

Chair of Committee,	David Russell
Committee Members,	Martin Dickman
	Emile Schweikert
	James Batteas
Head of Department,	Simon North

May 2016

Major Subject: Chemistry

ABSTRACT

With the trend in miniaturization in scientific research, nanomaterial use in various disciplines has become widespread. Proteomic research is a distinct area beginning to utilize nanomaterials for different research methods. There are several issues inherent to nanomaterials use that must be overcome to ensure their widespread use is successful in proteomics based applications. Of these issues size control, surface chemistry control and applications efficiencies using nanomaterials are the most prominent issues hindering advancements. In current studies, nanoparticle synthesis utilizing polymer based encapsulation is a method that allows for a simple synthesis, size control, variety of surface chemistry, and still affords ionization efficiencies and enhancements on par with other nanoparticle syntheses. Therefore, polymer based encapsulation techniques are used throughout this study of nanomaterial based proteomic applications.

Application efficiencies for nanomaterials in proteomic methods is a two-fold process: analytical methods and proteomic methods. Initially in this study, ionization efficiencies are investigated in mass spectrometry based analytical methods when using polymer encapsulated nanoparticles. This study was performed to ensure there is no significant degradation in efficiency when introducing the encapsulating polymers onto the surface of the nanoparticle during synthesis. Results showed that polymer introduction onto the surface of the nanoparticles did not interfere or significantly degrade the efficiencies with the mass spectrometry based analysis of standard peptide based samples.

Based on these findings polymer encapsulated nanoparticles were exploited for experiments to enhance proteomic based research methods.

The polymer-encapsulated nanoparticles are also successfully utilized in applications for specific proteomic based methods that require a robust yet sensitive platform needed in the harsh environments common in proteomic based research. Specifically, these nanoparticles were shown to function as a selective capture platforms for posttranslational modifications on proteins and peptides commonly found in nature.

ACKNOWLEDGEMENTS

I would like to thank my committee for their guidance and support throughout the course of this research.

Thanks also go to my friends and colleagues and the department faculty and staff for making my time at Texas A&M University a great experience.

Finally, thanks to my mother and father for their encouragement and to my wife for her patience and love throughout the entire process.

TABLE OF CONTENTS

Page

LIST OF FIGURES

Page

LIST OF TABLES

Page

CHAPTER I

INTRODUCTION

Development of Mass Spectrometry Ionization

There have been many ionization techniques developed for mass spectrometry since J.J. Thomson first refined the technique. Some of these ionization techniques are very simple and others are more intricate; listed are a few examples of ionization techniques: electron impact[1], chemical ionization[2], fast atom bombardment (FAB)[3], electrospray ionization (ESI)[4], and matrix assisted laser desorption ionization (MALDI)[5]. The 2002 Nobel Prize in chemistry was awarded in part to John Fenn for the development of ESI-MS and Koichi Tanaka for the implementation of MALDI-MS for protein and large polymers[4,6]. Both of these techniques are commonly utilized ionization techniques today for biological and large polymeric molecules[7,8]. These two techniques are described as soft ionization techniques and their development has pushed mass spectrometry to the forefront of biological research as a tool for characterizing biological molecules specifically their primary, secondary, and tertiary structure.

Nanoparticles in Mass Spectrometry

Since Tanaka and coworkers showed in 1988 that proteins could be ionized using fine metal powders consisting of 30 nm cobalt nanoparticles, there has been interest in using other nanoparticles for LDI-MS[6]. Nanoparticles that have been studied for various uses include: Fe_3O_4[9, 10], TiO_2[11], Ag[12], Au[13,14] , and SiO_2[15]. This technique is often times

referred to as surface assisted laser desorption ionization (SALDI), but for this report it will be referred to as laser desorption ionization (LDI). Nanoparticles offer several benefits when being utilized as platforms for LDI-MS: i) high surface area, ii) low interference in the mass-to-charge region of interest, and iii) ability to change the nanoparticle surface chemistry. The most notable impact that nanoparticles have in mass spectrometry applications is the high surface area, which allows more analyte molecules to directly interact with the surface of the nanoparticles. These nanoparticle surface analyte interactions should allow more analyte molecules to be ejected off the surface during the energy deposition/analyte ejection process. Nanoparticles (NPs) have also been used to analyze a wide variety of samples such as small molecules and biological molecules (i.e. proteins and peptides) because of the NPs low interference in the low molecular weight region[14]. The ability to control the surface chemistry of the NPs also permits cleaner ionization of target molecules[16, 17].

Modification of nanoparticles has been shown for several different types of nanoparticles such as AuNPs[16] and Fe_3O_4[10]. In recent years, AuNPs have received a lot of attention for their use in LDI-MS because of a simple synthesis (citrate reduction[18] and the method described by Brust et al.[19]), ease of altering the surface chemistry using ligands through thiol chemistry[16], and their ability to absorb laser energy at differing wavelengths based on size and shape[20]. Specifically, AuNPs that are modified using thiol chemistry to attach 4-aminothiol phenol (4-ATP) allowing the AuNPs to provide more protons for the ionization process which increased the mass range the AuNPs were capable of analyzing[21]. For example, Castellana and coworkers demonstrated similar chemistry applied to gold

nanorods (AuNR)[20]. Using 4-ATP modified AuNRs for LDI-MS demonstrates the ability to utilize different wavelengths of lasers to ionize analyte from the surface. Changing the shape of AuNPs to rods produces an absorption band, known as a surface plasmon resonance band[22,23], at different wavelengths than that of spherical AuNPs allowing for the use of different photon wavelengths to produce analyte signal during the LDI-MS experiment.

Proteomics and Mass Spectrometry

The study of proteins and their primary and modifications as well as their interaction with their surrounding is known as proteomics[24]. The task of isolating and characterizing all proteins is a considerable task to undertake given the number of proteins in a proteome, the range in the concentrations of the proteins and the possible isoforms that may be present. The advancements in mass spectrometry ionization techniques described by Karas and Hillencamp[5], Tanaka[6], and Fenn[4] have helped pushed mass spectrometry to the forefront of proteomic research. The soft ionization techniques combined with new developments in mass selections techniques have greatly increased the range, sensitivity, and resolution of mass spectrometers allowing them to be a valuable tool in proteomic studies. Many proteomic studies are conducted in following one of two experimental procedures: i) bottom-up and ii) top-down. Bottom-up utilizes an enzyme that will cleave proteins at certain residues producing peptides that are then analyzed using MS[7,25]. Bottom-up proteomics have challenges associated with analyzing samples that contain post translational modifications (PTM) such as ion suppression and loss of PTM.

Because of these challenges, techniques for enrichment of PTMs have been developed for several of the most commonly studied PTMs including phospho- and sulfo-peptides[26,27,28]. However, bottom-up proteomics have databases that allows for researchers to more easily identify proteins in the sample[7]. Another common proteomic strategy is top-down proteomics[29]. Top-down proteomics involves the analysis of intact proteins to determine the protein mass to charge ratio (m/z) followed by a fragmentation method that is carried out within the mass spectrometer to gain amino acid sequence information for the protein of interest[29]. This method allows for retention of post translational modifications and the possibility of greater sequence coverage due to the fragmentation occurring in the gas phase within the mass spectrometer. Top-down proteomics also has challenges present such as no readily available database for easy protein identification and the need for large quantities of isolated pure protein to allow for optimal results. Both of these methods have their benefits as well as short comings for use in proteomics. There have been several techniques developed to overcome some of these short comings especially for bottom-up approaches since this method allows for facile database searches for protein identification.

Translational Modification Enrichment

As with any field of research, there are limitations in proteomic studies; one such limitation is the handling and detection of post-translational modifications (PTM). Post-translational modifications are additions or deletions typically to specific residues within protein sequence that affect the properties of proteins typically through structural changes or function of the protein within the cell. These modifications have a dynamic range of

concentrations within the proteome and there are many types of modifications that are reversible and irreversible. Therefore, techniques are needed that are able to handle PTM in a bottom-up proteomics experiment. There have been several methods developed over the past few decades for selectively capturing some of these PTMs such as lectin affinity columns for glycosylation[30] and immobilized metal affinity chromatography (IMAC) for phosphorylation[31, 32]. These techniques along with many others used for PTM selective capture are chromatographic in nature requiring making and loading columns with the various chemical or metal ions. However, recently there have been many advances in these techniques that no longer involve columns.

Phosphorylation Tagging and Enrichment Techniques

Phosphorylation is one of the most common post translational modifications found throughout biology. Phosphorylation plays an important role in determining protein activity through phosphorylation and dephosphorylation of receptor sites that causes conformational changes in the site resulting in the "on" and "off" switching of the protein activity. An estimated ~40% of all proteins in eukaryotic cells are phosphorylated at any specific time, and of the ~40% of proteins that are phosphorylated there are an estimated 100,000 possible sites for modification in the mammalian proteome[33]. As mentioned above, the detection of PTMs such as phosphorylation is a difficult task due to the number of possible modification sites and dynamic range in concentration with the modification from protein to protein. Several enrichment techniques have been developed for more efficient detection of phospho-modified peptides and proteins. Of these enrichment

techniques, several of them require labeling of the modification with tags that allow for enrichment of the peptides/proteins. First, labeling-based enrichment techniques including β elimination/Michael addition[34] and phosphoramidate chemistry[35] are a few of the more well studied of these techniques. Among these labeling techniques, the β elimination/Michael addition is the most commonly employed; this technique is only applicable for phosphoserine (pSer) and phosphothreonine (pThr)[34]. The technique involves the elimination of the phosphate group from the amino acid side chain, using highly basic conditions producing the dehydroalanine derivative from pSer and β-methyldehydroalanine derivative from pThr. These derivatives then serve as a Michael acceptor, allowing for the attachment of a nucleophile for enrichment. A technique that has become more popular in recent years is phosphoramidate chemistry (PAC) based enrichment which was developed based on derivatization schemes for nucleotides[36]. PAC based enrichment is applicable to all commonly modified amino acids phosphoserine, phosphothreonine, and phosphotyrosine, while PAC allows for enrichment of all known phospho- modified amino acids. PAC method requires several preliminary steps before enrichment can be carried out. Specifically, all amines and carboxyl groups require modification to block as many false positive tagging events as possible, prior to tagging the phosphate groups. Following the derivatization of the phosphate groups, there are several enrichment methods that can be used including IMAC[37] and more recently the derivatization step is carried out using amine terminated polyaminoamide dendrimers (PAMAM)[36]. Using dendrimers allows enrichment based on size exclusion techniques. These two specific examples, along with other chemical based tagging methods are ways

to create derivatives that are specific for pSer, pThr, and pTyr, which allow for the enrichment of the phospho- modified peptide/ protein.

The enrichment of phosphopeptides/proteins through affinity methods such as IMAC[38], titanium dioxide MOAC[39], and strong cation exchange (SCX)[40] without derivatization of the peptides/proteins prior to enrichment has also been described. Immobilized metal affinity chromatography (IMAC) is the most commonly used technique for the enrichment of phosphopeptides/proteins in an offline based column format in modern proteomic research. With IMAC positively charged metal ions, such as Fe^{3+} [31] or Ga^{3+} [41], are coordinated to the surface of a solid phase resin through metal ion chelators, typically nitilotriacetic or iminodiacetic acid. Following the coordination of metal ions, the now positively charged resin is subjected to the negatively charged phosphoryl groups that captures the metal ions through electrostatic interactions. MOAC is an enrichment method for phosphopeptides/proteins that is similar to IMAC, but in place of metal ions being loaded into the surface of resin beads are metal oxides such as TiO_2[11]. Another method for enrichment that is specifically used phosphopeptides is strong cation exchange (SCX)[42]. This enrichment method also utilizes the interaction of a positively charged column with the negatively charged phosphate groups. To achieve separation of peptides from the column, phosphopeptides and nonphosphopeptides, the elution of peptides off the surface is done by changing the isoelectric point (pI). These methods are examples of many that have been described for the selective enrichment of phosphopeptides/proteins through affinity interactions. These techniques being both

online and offline chromatographic techniques, lend themselves to use for proteomic studies where mass spectrometry is used as a detection method.

Oxidized Cysteine Enrichment

Cysteine is a very important amino acid in the function of proteins due to it reactive thiol side chain, –SH. The thiol functionality allows for the oxidation and reduction of proteins to help control the activity in transduction pathways within cells[43-45]. The formation of sulfenic acid (R-SOH) and sulfinic acid ($R\text{-}SO_2H$) are oxidation products found in cells that are reversible, and they allow cells to process hydrogen peroxide or alky hydroperoxides to non-reactive species that will not damage the cells[46]. While these two products are reversible, there is a third product of oxidation to cysteine, sulfonic acid ($R\text{-}SO_3H$). Sulfonic acid modified cysteines have undergone several steps of oxidation to produce an irreversible oxidized stated of cysteine[47]. While the reversible oxidation states of cysteine are important, they are very difficult to trap due to their reversibility. However, the irreversibly modified sulfonic acid cysteines (cysteic acid) provide a simpler target for detection of oxidation sites within proteins. Methods have been developed for the capture of cysteic acid that included the use of antibodies[48] and modified nanodiamonds[28]. The technique developed using nanodiamonds is based on electrostatic interaction of positively charged nanodiamonds. Briefly, the surfaces of nanodiamonds are modified with polyarginine using several steps of EDC/NHS coupling[28]. Following the surface modification, peptide mixtures and protein digests containing cysteic acid modification

are captured on the surface through electrostatic interactions and then subjected mass analysis through MALDI-MS[28].

Nanoparticles in Post Translational Modification Enrichment

Recently, nanoparticles of various types have been studied for use in PTM enrichment as an alternative to traditional chromatographic techniques used for these enrichments. Nanoparticles used in the enrichment of PTMs vary from Fe_3O_4 to gold nanoparticles (AuNPs). The simplest nanoparticle enrichment scheme is using the nanoparticles as synthesized without any modifications to enrich post translational modifications. This enrichment scheme has been done using TiO_2 for direct phosphopeptide enrichment[49] and using AuNPs for the enrichment of thiol containing compounds, such as cysteine containing peptides through direct interaction with the nanoparticle surface[50]. While these methods are the simplest and a common use of nanoparticles in the enrichment of PTMs, altering the surface chemistry of the nanoparticles to allow for efficient enrichment of specific PTMs can also be used. These modifications can include various non-covalent binding motifs for PTMs such as antibodies or metal binding ligand[48]. Antibodies have been coupled to magnetic nanoparticles for their use in a human plasma immunoassay[51]. Magnetic nanoparticles have also had metal chelating ligands, such as those used in traditional IMAC, attached for the selective enrichment of both His-tagged proteins and phosphorylated peptides[52]. Other nonmagnetic nanoparticles have also been modified for non-covalent enrichment,

including AuNPs. Specifically, gold nanorods (AuNR) have been modified with lipid layers to capture myristoyl modified peptides and other membrane active molecules[13].

Polymers Used for AuNP Synthesis

Recently, synthesis of metal nanoparticles with polymers has been gaining significant interest. Polymers such as: PAMAM dendrimers[53], PMMA,[54], PNIPAM[55], PVP[56], and various block copolymers[57] have been used in these systems as they offer a surface that is biologically compatible and stabilizes the NPs for long periods of time, these characteristics are crucial for NPs use in biological studies. The polymer/NP systems have been studied in applications for: drug delivery[58], surface enhanced Raman studies (SERS)[59], and use in thin film development using NPs[60,61,57]. One polymer that has been used of particular interest for this report is poly(4-vinylpyridine) P4VP This polymer allows synthesis of polymer encapsulated AuNPs with a narrow size distribution that are stable in solution for long periods of time[61]. Pyridine groups on the back bone of the polymer interact with the surface of the AuNP encapsulating these AuNPs in the polymer following reduction of $HAuCl_4$ in solution (**Scheme 1**). There are free pyridine pendant groups that are not bound to the surface, and these pyridines have been shown to hydrogen bond to acidic polymers, lending to a method for layer formation with AuNPs embedded in the layers[61]. Along with P4VP, another polymer system that has been used for NP synthesis is PAMAM dendrimers[62]. Dendrimers allow for a simple one pot synthesis that has the advantage of controlling the size of the NPs while also providing a platform that is stable and ridged. The dendrimers allow for controlling the surface

chemistry through post NP synthesis functionalization by simple chemical coupling reactions with the terminal groups on the dendrimer arms that can provide essential function for the dendrimer NP complexes such as use in posttranslational modified peptide capture[63,64].

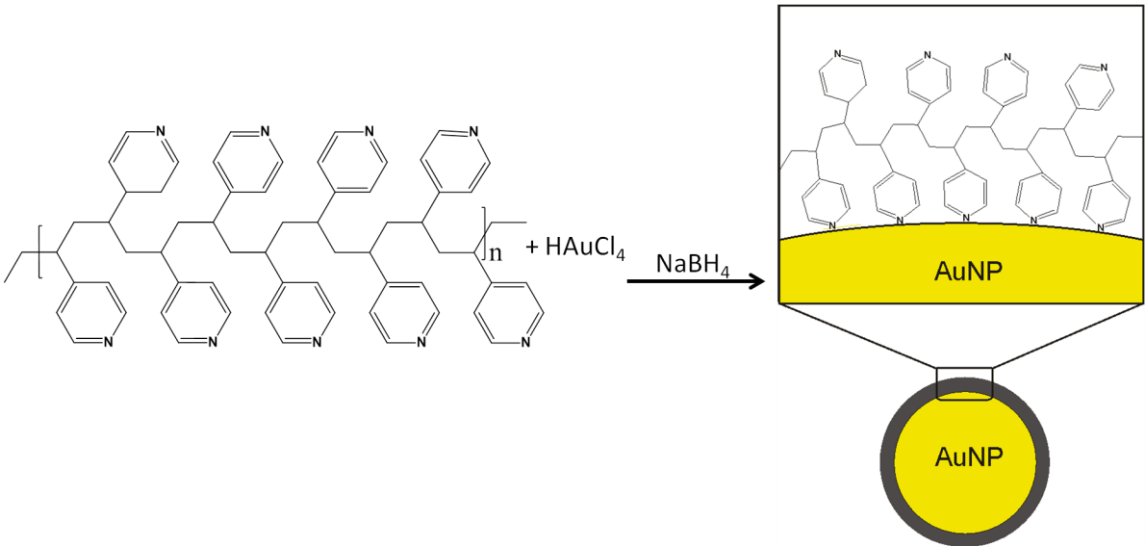

Scheme 1. Synthetic scheme for poly(4-vinylpyridiene)(P4VP) encapsulates AuNPs.

CHAPTER II

POLYMER ENCAPSULATED GOLD NANOPARTICLES USED FOR LDI-MS: AN INVESTIGATION OF THE EFFECTS OF PEPTIDE INTERACTIONS WITH THE SURFACE ON IONIZATION EFFICIENCY

Introduction

The interest in utilizing nanoparticles as a matrix for LDI-MS began with Tanaka and coworkers, who showed that biological molecules and large polymers can be ionized using fine powders consisting of 30 nm cobalt nanoparticles[6]. Subsequently, a variety of nanoparticles[12,14,16,65-71] have been investigated as potential matrices for LDI-MS, and have allowed for the study of a wide variety of analytes in LDI-MS. For example, small molecules using SiO_2 NPs[15], biological molecules (proteins and peptides) using AuNPs[68], and AgNPs have been used to selectively ionize molecules such as the analysis of olefins and cholesterol [12]. In recent years, AuNPs have received increased attention for their use in LDI-MS owing to the ease of AuNPs synthesis which allows for great control of size, particle shape, and the ability to alter the surface chemistry of the nanoparticles after synthesis with simple ligand exchange [72]. AuNPs can be synthesized to create an array of shapes which can lead to distinct optical properties further exploiting their capabilities for LDI-MS by allowing for various laser wavelengths to be used.

Although the ability to synthesize AuNPs with controllable optical properties is relatively straightforward, there are difficulties associated with using AuNPs for use in mass spectrometry (MS) analysis. Our lab has previously shown that salts and other

contaminates present in the samples, either from the analytes or AuNPs, greatly affect the LDI ion yields for analytes in both the positive and negative ion mode[67]. The primary concern is that the synthesis of AuNPs is "dirty", resulting in several species present that are not conducive to MS analysis owing to interactions with the AuNP or the analytes. The standard synthesis of AuNPs relies on using sodium citrate as a protecting agent for the AuNPs; the electrostatic interaction between the citrate and the AuNPs prevents the particles from aggregating to form larger particles. The adverse effects citrate has on ion yields in mass spectrometry can be overcome by displacing citrate from the AuNPs with protecting agents such as 4-aminothiolphenol (4-ATP) [68], either during synthesis or subsequently by ligand exchange. The physical interaction the protecting agents have with the AuNPs is important to consider when using AuNPs to desorb/ionize analytes from the surface. Changing the surface properties of AuNPs by altering the ligands used to stabilize the NPs can lead to cleaner spectra as well as enhance the ionization of biological molecules. Altering the surface chemistry by using a molecule such as 4-ATP provides enhanced ionization efficiency for peptides and allows for ionization of proteins [68]. Our lab has recently illustrated that changing the shape of the AuNP can facilitate ionization of biologically relevant molecules using different wavelength lasers[20]. Furthermore, it has been demonstrated that alternate shapes of gold nanomaterials can be used to enrich specific analytes from complex mixture[13]. The physical interaction between protecting agents and analytes as well as the chemical properties of the protecting agent are important to consider when using AuNPs for LDI-MS.

Based on previous results, the use of alternative protecting agents could hold utility for synthesis of AuNPs and for use in LDI-MS. The use of various polymers as protecting agents on the surface AuNPs has been studied extensively because of their ability to stabilize the NPs through multiple interactions between the surface of the nanoparticles and the polymers. Polymer protecting agents are attractive for use as protecting agents because the passivation of the AuNPs with polymers affords improved stability of the particles for long periods of time through various types of interactions with the surface. Several polymers have been used to encapsulate nanoparticles including poly(N-isopropylacrylamide) (PNIPAM)[55], poly(4-vinylpyridine) (P4VP)[17,61], poly(methyl methacrylate) (PMMA)[54], poly(vinylpyrrolidone) (PVP)[56], and DNA[73]. Block co-polymers have also been used as protecting agents for AuNPs such as poly(ethyleneoxide)-polystyrene (PEO-PS)[60] and polystyrene-b-poly(-vinylpyridine) (PS-b-PVP)[74,75]. Using polymers as protecting agents for AuNPs allows for the tailoring of the surface of the NPs to be altered in a manner that the AuNP polymer complex becomes useful in biological systems. Examples of this are pH responsive polymers allowing the AuNPs to aggregates[76], and polymers that can be used to deliver molecules through temperature induced changes in the polymers themselves[77]. Polymers that have the ability to interact with analytes in a similar fashion to other organic molecules could provide an enhancement in ionization of peptides from LDI-MS utilizing encapsulated AuNPs and could serve as a viable matrix in mass spectrometry.

In this study, we aim to gain a better understanding of how the surface of nanoparticles functionalized with poly (4-vinylpyridine) interacts with peptides and how

these interactions, or lack thereof, will effect ionization efficiencies of the peptides in LDI-MS. To accomplish this we use P4VP to synthesize polymer encapsulated AuNPs (P4VP/AuNPs) with a narrow size distribution that are stable in solution for several weeks. Pyridine groups on the backbone of the polymer interact with the surface of the AuNP encapsulating these particles following reduction of HAuCl4 in solution. Some of the pyridine units will have no direct interaction with the AuNP surface, and they can interact with other molecules suspended in the solution. We demonstrate that using a polymer as a protecting agent on AuNPs is straightforward and provides a simple method to circumvent the contamination problems associated with commercially available citrate capped AuNPs when considering their use in LDI-MS. Finally, we show that P4VP/AuNPs lead to enhanced ionization efficiencies for peptides when compared to citrate capped AuNPs similar to those previously studied[68].

Experimental

Materials

Hydrogen tetrachloroaurate (III) ($HAuCl_4$), poly(4-vinylpyridine) (P4VP), trifluoroacetic acid (TFA), methanol (MeOH), ammonium acetate, formic acid (FA), and trifluoroethanol (TFE) were purchased from Sigma Aldrich (St. Louis, MO). Sodium borohydride ($NaBH_4$) was purchased from EMD Chemicals Inc. (Darmstadt, Germany). Citrate capped gold nanoparticles, and 400 mesh carbon coated copper grids were obtained from Ted Pella Inc. (Redding, CA). The peptides [Val4] angiotensin III (RVYVHPF),

human ACTH clip 6-24 (HPRWGKPVFKKRRPVKVYP), C-telopeptide (ELAHDGGR), angiotensin II (DRVYIHPF), and neurotensin (Glp-LYENKPRRPYIL) were purchased from American Peptide Company Inc. (Sunnyvale, CA). Molecular weight cutoff filters (MWCO) 100 kDa and 10 kDa, as well as Milli-Q water were obtained from Millipore Corp. (Bedford, MA). All reagents and peptides were used as received without further purification.

AuNP Preparation

AuNP's were synthesized using the method previously published by Hao *et al*[61]. The reaction scheme is depicted in **Scheme 2**. After the P4VP/AuNPs were synthesized, the sample was lyophylized to dryness to remove the solvent and the remaining solid pellets were washed twice using 500 µL of 18 MΩ water, then resuspended in 0.1% TFA followed by sonication. The resulting solution was further purified using MWCO filters of 100 kDa, and the solution volume was reduced to one tenth the initial volume in 0.1% TFA at the end of purification.

Characterization

P4VP/AuNPs were characterized using two different methods: (i) UV-Vis spectroscopy and (ii) transmission electron microscopy (TEM). For the UV-Vis characterization an Agilent 8453 UV-Vis spectrometer (Agilent Technologies, Santa Clara, CA) was used. The UV-Vis spectrum was acquired from 200nm to 900nm using a 1:3 (P4VP/AuNP:MeOH) dilution in a 1 cm quartz cuvette. TEM was carried out by

spotting 1 µL of the AuNP synthesis solution on a 400 mesh carbon coated copper grids with a JOEL JEM 2010 (Peabody, MA) microscope at 200 kV. The X-ray photoelectron spectroscopy (XPS) was performed on a Kratos Axis Ultra Imaging X-ray photoelectron spectrometer using mono Al source (Kratos Analytical, Manchester, United Kingdom).

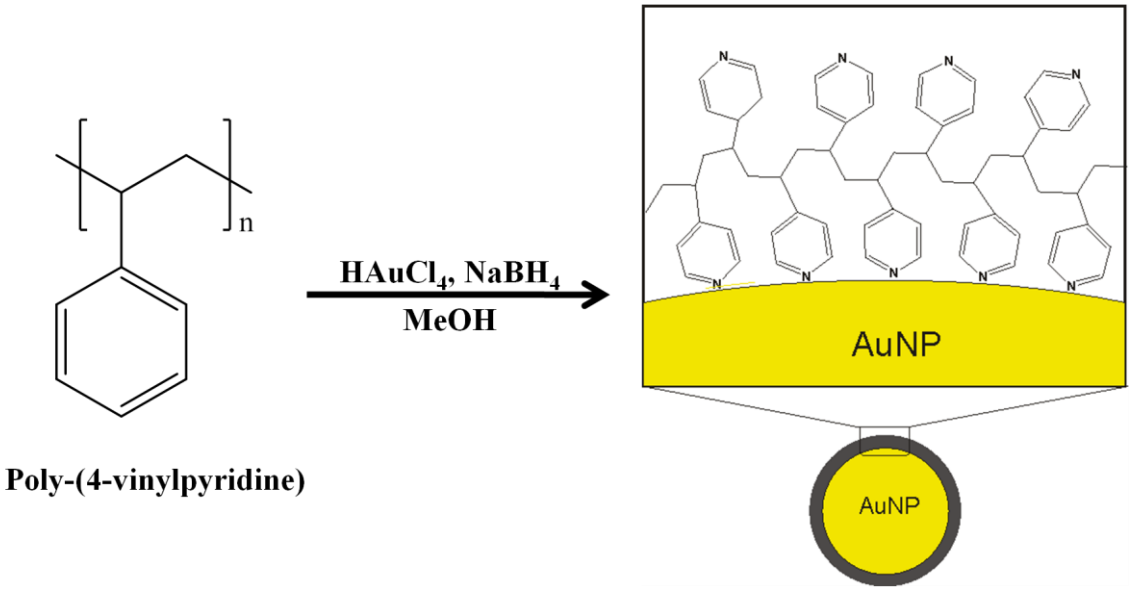

Poly-(4-vinylpyridine)

Scheme 2. Reaction scheme for the production of P4VP encapsulated AuNPs. The right hand side of the scheme depicts the AuNP coated in polymer with pyridine subunits not interacting with the surface of the NP, leading to free pyridine subunits.

Preparation and Laser Desorption/Ionization (LDI)

Serial dilution of peptide stock solutions (1mg/1mL) was used to obtain a range of analyte concentrations for this study. Peptides were mixed directly with either the commercially available citrate capped AuNPs or P4VP/AuNPs, at the ratio: 1 µL of peptide was mixed with 9 µL of AuNP solution. Final concentrations of the peptides used in this study after mixing with the AuNP solutions were 100 µM, 75 µM, 50 µM, 25 µM,

10 μM, 7.5 μM, 5 μM, 2.5 μM, and 1 μM. One microliter of the resulting mixture was then spotted onto a stainless steel MALDI plate and the spots were dried using a speed vacuum. All samples were analyzed using a Voyager - DE STR (Applied Biosystems, Framingham, MA) in the positive ion reflected mode using a 337 nm laser with an acceleration voltage of 20 kV, grid voltage of 67%, delay time of 200 nsec, and ~9 μJ per laser shot.

Results and Discussion

In this work we incorporate a polymer-based method to synthesize AuNPs, in which the particle size is controlled and can be used to facilitate LDI-MS. The synthesis of the poly(4-vinylpyridine) (P4VP) encapsulated AuNPs (P4VP/AuNPs). This provided a wine red solution typical of a gold colloidal solution consisting of particles larger than 2 nm in diameter. To characterize the resulting, P4VP/AuNPs, UV-Vis spectroscopy, transmission electron microscopy (TEM), and x-ray photoelectron spectroscopy (XPS) were used. The UV-Vis spectrum (**Figure 1a**) exhibits two absorbance maximums; **(i)** The peak at 250 nm corresponds to the polymer specific to the pyridine groups, and **(ii)** the 520 nm absorbance is characteristic of AuNPs, larger than 2 nm in diameter, consistent with the color of the AuNP solution. To confirm the size of the AuNPs, TEM images were obtained (**Figure 1b)** and the average size distribution was determined to be 2.4 ± 0.6 nm. The size is important to consider when using P4VP/AuNPs for LDI-MS, as it has been shown that 5 nm AuNPs yields higher relative abundances of peptide ions compared to the use of smaller (< 2 nm) and larger (> 10 nm) AuNPs.

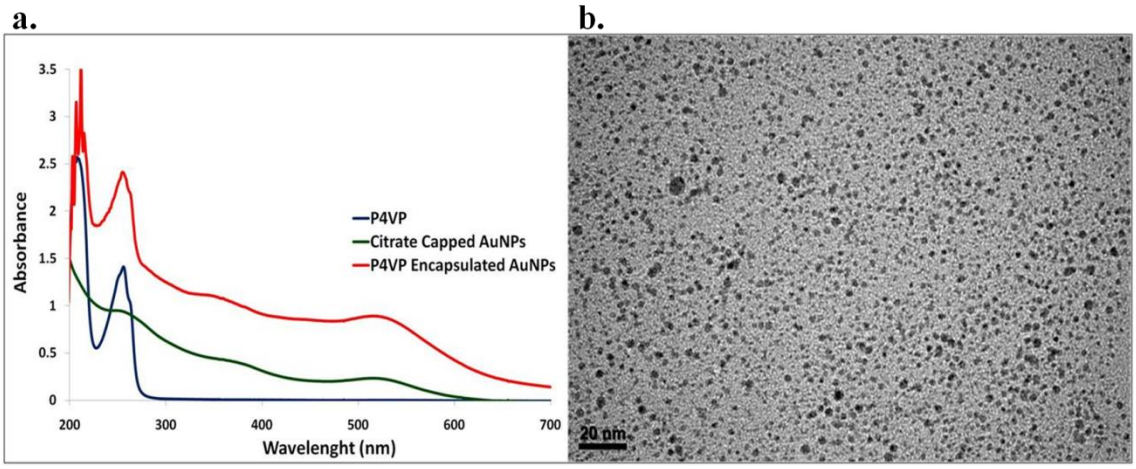

Figure 1. a. Characteristic UV-Vis spectra for P4VP encapsulated AuNPs with an absorbance at 520 nm and 250 nm representing AuNPs and P4VP. b. TEM image at 100k magnification of P4VP AuNPs. Average size distribution is 2.4 ± 0.6 nm.

XPS analysis was run on the P4VP/AuNPs to better determine the surface chemistry of the AuNPs. The high resolution scan of the nitrogen 1s electron binding energies displays two peaks at 399.8 eV and 402.4 eV, **Figure 2a**. The two peaks correspond to the two different types of pyridyl nitrogens present in the sample. The first of the nitrogen peaks is due to interaction with the surface of the AuNPs. The second nitrogen peak is due to the lack of surface interaction; therefore, has a binding energy. High resolution scans of gold 4f electrons were also performed on the same sample and displays two peaks that correspond with known gold 4f electron binding energies, **Figure 2b.**

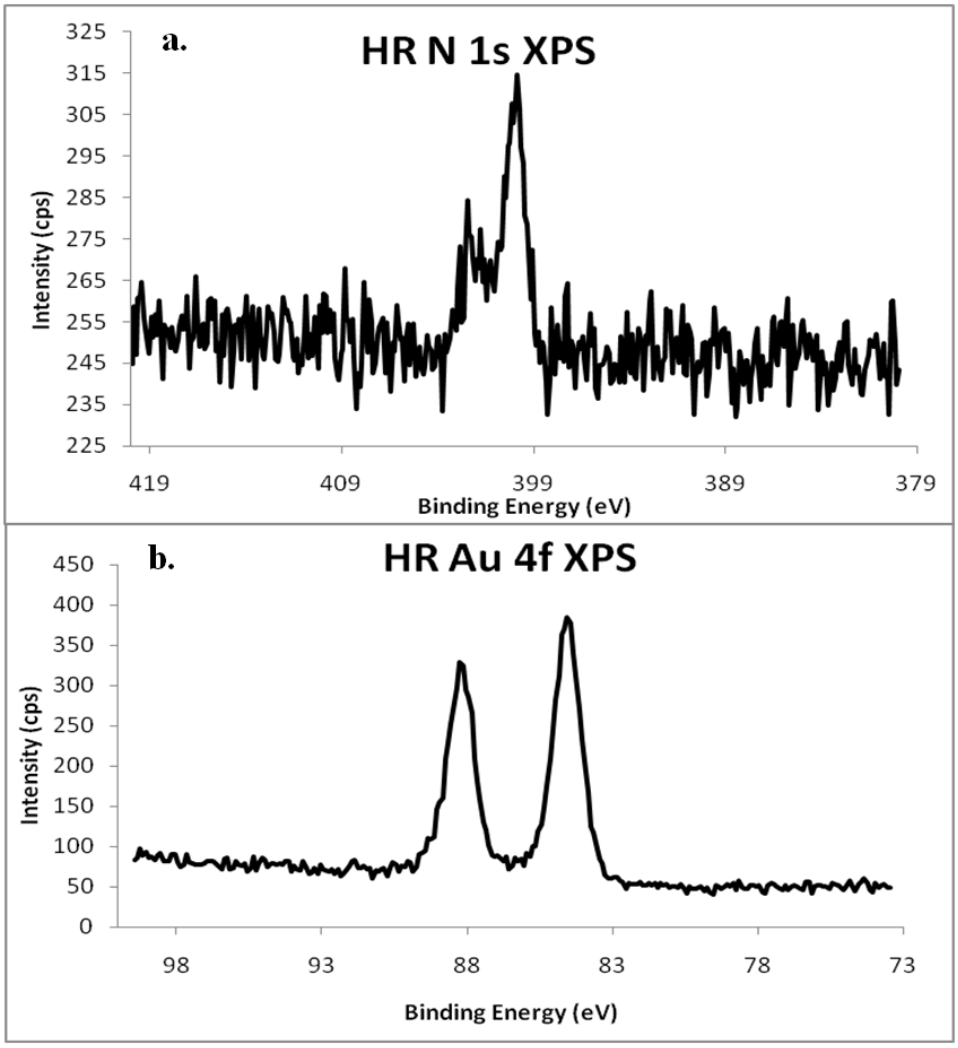

Figure 2. a. High resolution nitrogen 1s electron x-ray photoelectron spectrum taken from P4VP/AuNPs. b. High resolution gold 4f electron x-ray photoelectron spectrum taken from P4VP/AuNPs.

Following the characterization of the AuNPs, we conducted experiments with peptides using P4VP/AuNPs in LDI-MS to determine the viability of these P4VP/AuNPs. A number of peptides were examined including human ACTH clip 18-39 (RPVKVYPNGAEDESAEAFPLEF) and [Val4] Angiotensin III (RVYVHPF), in which

representative spectra for both peptides are provided in **Figure 3a** and **3b** respectively. LDI-MS of each peptide was also performed in the absence of P4VP/AuNPs, in which no analyte signal was observed at the same laser energies and peptide concentration used to analyze the peptide P4VP/AuNP mixture. Additionally we compared the peptide ionization efficiencies of P4VP/AuNPs to citrate capped AuNPs. Higher laser fluence was required when using the citrate capped AuNPs to achieve desorption/ionization of the peptides examined. Moreover, the most abundant ion signal in the spectra for the peptides analyzed with the citrate capped AuNPs was the $[M+Na]^+$ ion whereas analysis using P4VP/AuNPs resulted in the $[M+H]^+$ ion being the predominate ion signal observed. The high abundance of the $[M+Na]^+$ and $[M+K]^+$ ions when using the commercially available AuNPs can be explained by the presence of alkali metals which act as counter ions to the citrate group, which is used as the capping agent during the synthesis. The presence of alkali metals in the citrate capped AuNPs has been shown to be a possible drawback to MS analysis because of the formation of alkali adducts. Conversely, there is little alkali metal present in the synthesis of P4VP/AuNPs, and through a centrifugation cleanup procedure performed before using in LDI-MS experiments, a majority of the residual alkali metals are removed. The final step in the cleanup process utilizes diluting the P4VP/AuNPs in an acid solution.

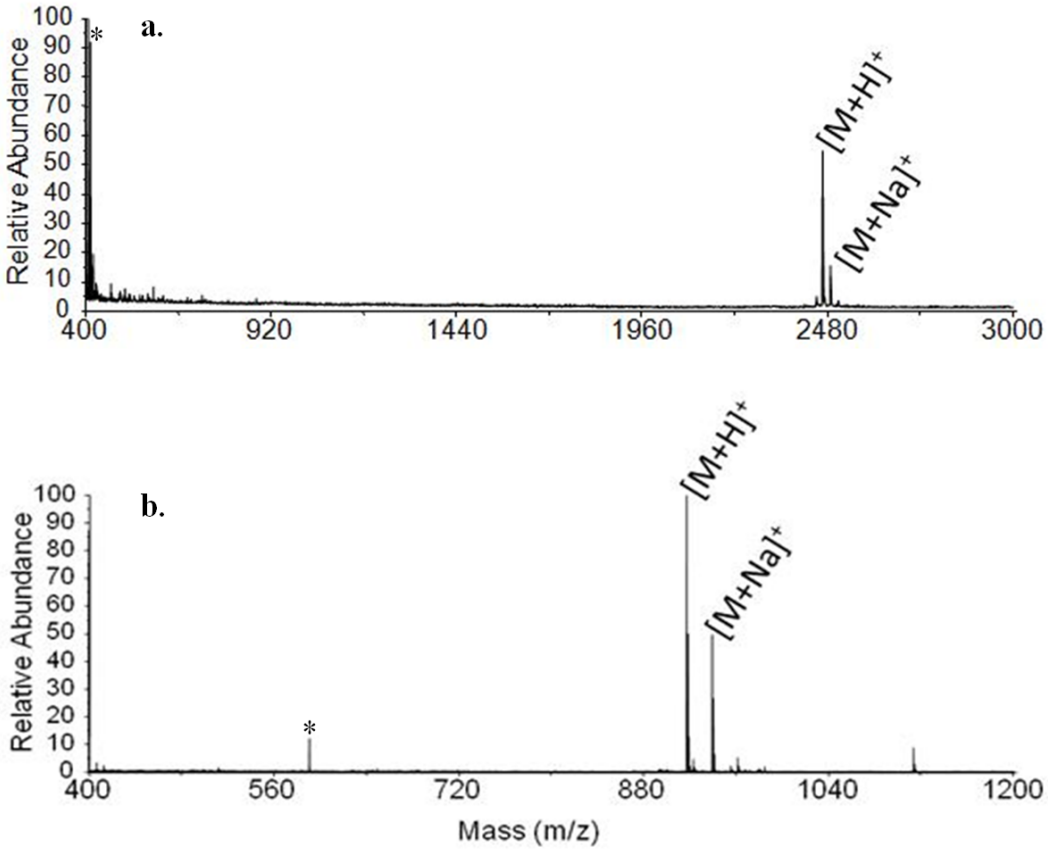

Figure 3. a. LDI-MS spectrum of Val[4]Angiotension III, RVYVHPF m/z 916.5, with P4VP encapsulated AuNPs. The $[M+H\}^+$ and $[M+Na]^+$ are observed as predominate peaks in the spectrum. b. LDI-MS spectrum of human ACTH (18-39), RPVKVYPNGAIDESAEAFPLEF m/z 2465.2, with P4VP encapsulated AuNPs. Observed peaks in the spectra that are characteristic of the polymer NP complex (*), the $[M+H]^+$ and $[M+Na]^+$ are observed for the analyte.

It is also important to note that through the synthesis there will be pyridine subunits that do not interact with the surface of the AuNP, see **Scheme 1**. The addition of acid leads to protonation of the free pyridines, which helps solubilize the P4VP/AuNPs and provides a source of protons during the laser desorption experiment. Low abundance signals of the alkali metal adducted peptides could result from alkali contaminates in the peptide

solutions. It should also be noted there are no interference peaks from the polymer in the mass range observed in the spectra seen in **Figure 3b**.

Once it was determined P4VP/AuNPs were capable of generating protonated signal for peptides a range of peptides were studied. These peptides had differing amino acid sequences and varying isoelectric points (pI); results of these studies can be seen in **Figure 4**. When studying the various peptides patterns are observed for angiotensin II and human ACTH clip (6-24) which show an increase in ion counts for these peptides as the amount spotted decreases to 75 picomoles, **Figure 4a** and **Figure 4d**. Following this increase there is a decrease in ion counts until there is no signal detected for these peptides. One possible rationalization for this observation is that the size and ring structure of the side chains (i.e. phenylalanine, histidine, tyrosine, proline, and tryptophan), which effects folding of the peptide, could directly interact with the P4VP/AuNPs. This interaction could alter the distance between the AuNP resulting in changes to desorption and ionization process for the peptides. Since the AuNPs are absorbing the photons and transferring their energy to the peptides for desorption, this interaction is extremely important to consider. If this interaction causes the peptides to exist at a distance in which the peptide will no longer feel the effects of the AuNPs desorption process, then the peptides will presumably not be desorbed off the surface. Alternatively if multiple side chains of the peptide interact with the polymer or surface of the AuNPs, the interaction could be strong enough that the peptide may not be desorbed off the surface. Interactions

between proteins, peptides and nanoparticles have been previously described wherein the binding energy and structure of the protein or peptide changes due to the interactions[78-81].

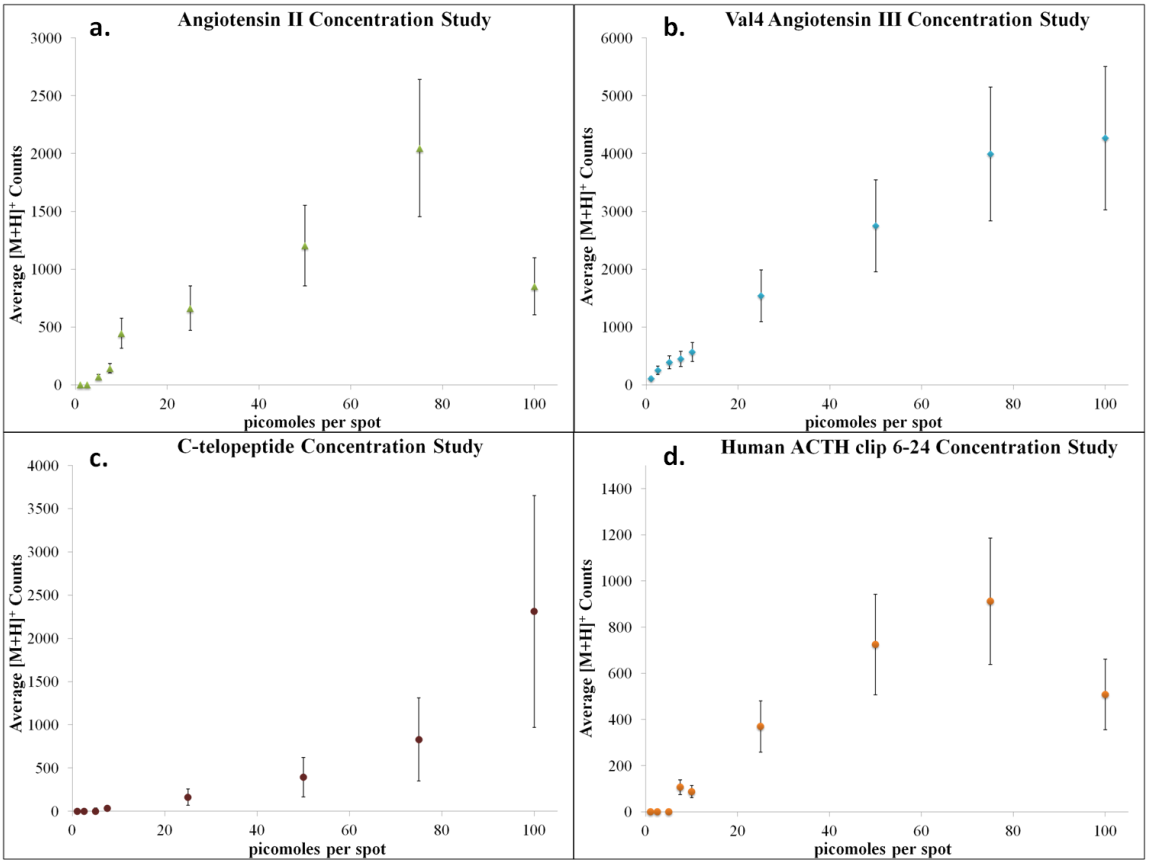

Figure 4. Graphs that present the concentration of peptide vs. average ion counts for [M+H]+. The peptides are a. angiotensin II (DRVYIHPF) m/z 1046.5, pI 6.74, b. Val4Angiotensin III (RVYVHPF) m/z 917.1, pI 8.75, c. C-telopeptide (EKAHDGGR) m/z 868.9, pI 6.85, and d. human ACTH clip (6-24) (HFRWGKPVGKKRRPVKVYP) m/z 2335.9, pI 11.75. All error bars are in the form of percent error.

Two interactions that could be affecting the ionization efficiency of angiotensin II (**Figure 4a**) and human ACTH clip 6-24 (**Figure 4d**) could be electrostatic or hydrophobic stacking with the polymer on the surface of the P4VP/AuNPs. To test this theory, we

compared angiotensin II which contains four amino acids considered to be large hydrophobic side chains (Tyr, His, Phe, etc…), to C-telopeptide which has one such amino acid (His). We predict that C-telopeptide should have higher ionization efficiency, which data in **Figure 4c** confirms. As the amount of peptide deposited with the nanoparticles decreases, the angiotensin II signal begins to show an increase in the ionization efficiency before it too begins to decrease. This trend could is suggestive that hydrophobic interaction through pi stacking with the polymer has a significant effect on the ionization efficiency. One conclusion is as the concentration of peptide within the spot increases, layers of peptide buildup on to the surface of the P4VP/AuNPs due to the hydrophobic interactions until the loading of the peptide reaches a maximum capacity. Once this capacity has been exceeded not all of the peptide can be desorbed/ionized off the surface of the AuNPs, causing the lowered ionization efficiency at higher concentrations. Another conclusion is that electrostatic interactions could be very strong through several side chain polymer interactions causing the peptides to not be desorbed off the surface of the AuNPs. This seems unlikely, as the peptides seem to recover ionization efficiency once the concentration has been lowered and the pH of the solution suggests that all peptide and polymer charge sites will be protonated, lowering interaction potential. We wanted to investigate whether or not these peptide interactions with the AuNPs were actually causing the signal reduction at higher peptide concentrations. In order to accomplish this, we altered the solvent conditions, with the hopes that changing the solvent would change the interactions the peptides might have with the P4VP/AuNPs, in which the peptides were dissolved before mixing with the AuNPs.

The study of the effect of solvent was carried out using a peptide that contains several amino acids with side chains that are large and can interact with the polymer layer on the AuNPs as well as side chains that can be easily protonated, human ACTH clip 6-24. This peptide also follows the trend of increasing ionization efficiency as the concentration decreased until a certain point where the ionization efficiency begins to decrease (**Figure 4d**). To better understand which of these interactions could possibly cause this ionization efficiency trend we chose to use a buffer solution (ammonium acetate) and two different organic solvents (trifluoroethanol and methanol). The ammonium acetate (AA) trend line in **Figure 5** has the highest ionization efficiency for all of the solvents chosen. This can be attributed to the availability of protons in the mixture as the ammonium acetate was buffered using formic acid. The proton availability is important due to the binding energy of a hydrogen to a pyridyl nitrogen is ~900 kJ/mol therefore the ability of the peptide to strip a proton from these sites during the laser desorption and ionization process is low[82].

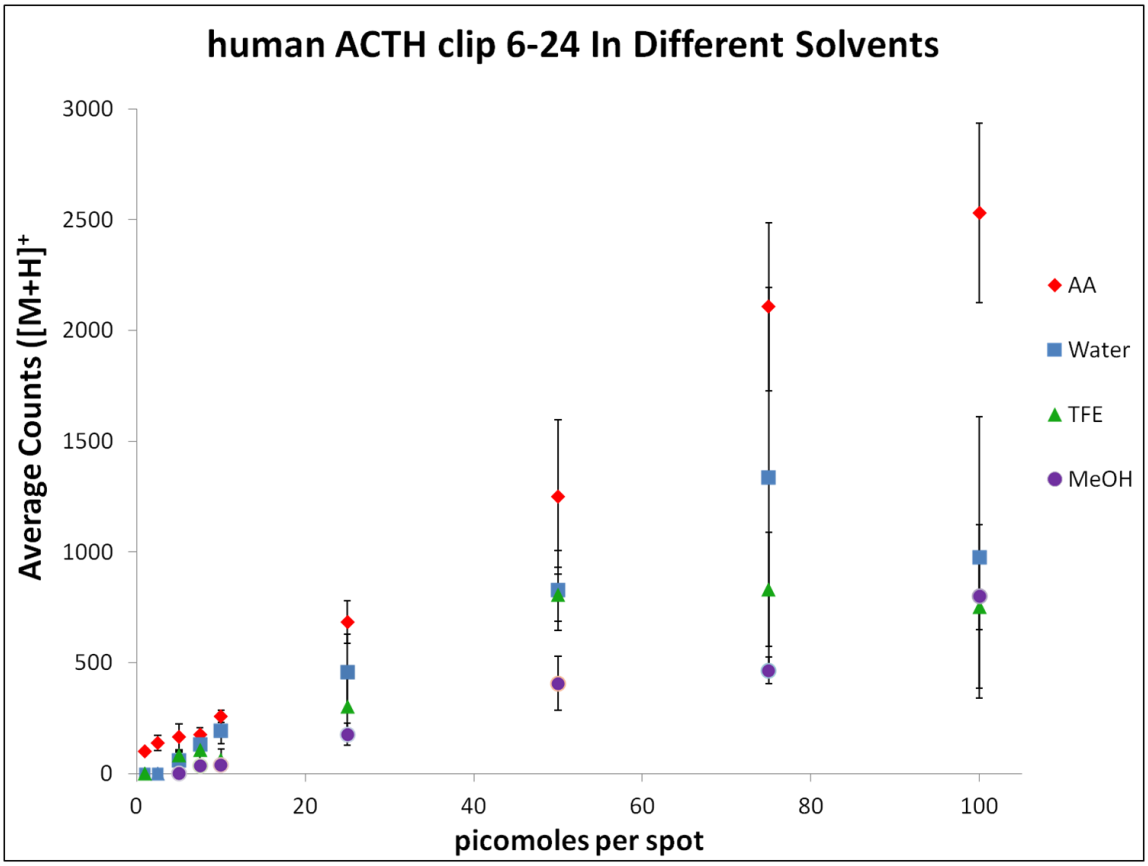

Figure 5. A plot containing a comparison between concentration of human ACTH clip (6-24)(HFRWGKPVGKKRRPVKVYP) m/z 2335.9, pI 11.75, vs. average ion counts $[M+H]^+$ in different solvent conditions. All error bars are in the form of percent error.

Thus, in this buffer solution the human ACTH clip 6-24 is more readily protonated as the peptide is not competing with the pyridine groups for the protons leading to an expected trend in ionization wherein the average $[M+H]^+$ counts decreases as the concentration decreases. Alternatively, the proton availability with the P4VP/AuNPs also leads to the lower ionization efficiency of human ACTH clip 6-24 in the other solvents shown in **Figure 5**. Trifluoroethanol (TFE) was investigated because of its ability to hydrogen bond

with the peptide and the pyridine group preventing any possible interactions between the peptide and the pyridine encapsulated AuNPs[83]. TFE can also preserve the secondary structure within proteins by reducing the hydrophobic interactions with other molecules of similar structure[83,84,85]. The data for TFE in **Figure 5** show that the ionization efficiency for the peptide is lower than that of the ammonium acetate and water but is similar to methanol. This lowered ionization efficiency could be a result of the peptide being protected by the TFE molecules that are hydrogen bonded both to the peptide as well as to the pyridyl nitrogens surrounding the AuNP. Hence the peptide will not be able to interact closely enough with the P4VP/AuNPs to either gain a proton from the pyridine, or is not able to interact with the AuNP in a manner that allows the peptide receive the energy deposited by the laser during the LDI-MS experiments. To further test the effects of the solvent we studied methanol because of its propensity to disrupt the hydrophobic interactions the peptide could have with the P4VP encapsulating the AuNPs without having as strong interactions as TFE. Since these two organic solvents display similar trends in ionization efficiency with human ACTH clip 6-24 (**Figure 5**), we can conclude that their ability to reduce the effect of hydrophobic interactions the peptide has with the P4VP/AuNPs. From these data we can determine that the major causes of the observed trends are twofold **a)** the availability of protons in the solution of the peptide and **b)** the hydrophobic interaction the peptide has with the P4VP/AuNPs.

Conclusion

With the focus of modern research trending toward biochemical issues, it is important to understand how molecules interact with surfaces, such as those of AuNPs and their protecting agents; this includes optimizing methods to analyze these molecules/systems. The use of poly(4-vinylpyridine) (P4VP) to synthesize AuNPs yields not only a small size distribution of AuNPs but incorporates a proton source into the system. Using P4VP/AuNPs for LDI-MS provides a similar platform to citrate capped AuNPs with few interference peaks observed in the mass spectrum. However, the polymer bound to the surface of the AuNPs reduces the presence of alkali metal adducts seen in the mass spectrum making P4VP/AuNPs a viable platform for peptide analysis through LDI-MS. Although, using P4VP/AuNPs have benefits over citrated capped AuNPs there are several things to consider about P4VP/AuNPs as an LDI-MS platform such as the interaction, hydrophobic and electrostatic, an analyte could have with polymer subunits and these interactions effect on ionization efficiency for the analyte. From this study we have demonstrated that the use of organic solvents to dissolve the peptide human ACTH clip 6-24 can disrupt the hydrophobic interactions between the amino acid side chains and the polymer subunits. This causes the ionization efficiencies to be lowered as a result of the decreased interaction with the AuNPs. Also involved in the lowering of the ionization efficiencies is the low availability of protons in the P4VP/AuNPs which could be an effect of the proton affinity of pyridine, which can be overcome by the solvent being used having excess protons incorporated within them. Therefore, we can conclude that solvent effects

on peptides interactions are important and proton availability is also very important to consider when using P4VP/AuNPs for LDI-MS of peptides.

CHAPTER III

POLY(4-VINYLPYRIDINE) ENCAPSULATED GOLD NANOPARTICLES AS AN ENRICHMENT METHOD FOR PHOSPHORYLATED PEPTIDES AND PROTEINS

Introduction

There are significant challenges in proteomic research associated with posttranslational modifications (PTMs). The dynamic range and complexity of the possible modifications has led to the development of methods that selectively capture specific functionalities of posttranslational modifications. Immobilized metal ion chromatography (IMAC) and metal oxide affinity chromatography (MOAC) for phosphorylation[86], lectin affinity chromatography for glycoproteins[30], and covalent chromatography for cysteine containing peptides[87] are examples of these functionality specific capture methods. More recently, there have been enrichment methods for subsets of peptides through labeling using facile bioaffinity tags[88]. These methods both coupled with mass spectrometry (MS) have overcome several of the challenges present in posttranslational modification proteomic research.

There has been a substantial research movement toward using nanomaterials for a variety of applications, specifically surface chemistry with applications in mass spectrometry[16,20,69,81,89-95]. The use of surface modified gold nanoparticles (AuNPs) for the ionization of biological molecules (proteins and peptides)[95,96], as well as silver nanoparticles (AgNPs) have been used to selectively ionize molecules such as the analysis of olefins and cholesterol[12]. With the advancement of nanomaterials in mass

spectrometry, the realm of possibilities of using functionalized nanomaterials for selective capture platforms has become a research interest in the field of proteomics[16,53,16,52,97-101]. One specific example wherein Lai et al.[38] synthesized magnetic Fe_3O_4 nanoparticles that are then functionalized post synthesis with standard metal coordinating molecules (NTA) used in IMAC columns. Following the synthesis and functionalization these magnetic nanoparticles are demonstrated capturing histidine tagged and phosphorylated peptides/proteins[38]. The demonstration of these surface modified nanoparticles opens the possibility for nanoparticles that need no further modifications before they are useful as selective capture platforms.

Nanoparticle synthesis is a large and highly researched field, and the synthesis of AuNPs is of particular interest to this research. Brust et al.[102] described the most common and widely used synthesis for AuNPs. This synthesis allows for control over the NP size through controlling the concentration of the reactants, and controlling the temperature the reaction is allowed to reflux[102]. Recently, there has been interest in the use of other capping agents for AuNPs that also allows for a simple one pot synthesis. Some of these capping agents are polymers such as PNIPAM[55], PAMAM dendrimers[36] (ref), and poly(4-vinylpyridine) (P4VP)[56]. P4VP is useful as a capping agent that allows for a one pot synthesis because it is an ionophore[56]. This allows the Au^{3+} ions to bind to the polymer before being reduced to form AuNPs that can be used to form layers of AuNPs within a polymer network[56]. The hydrogen bonding interactions used for building up layers allows us to extend the application of the P4VP encapsulated AuNPs (P4VP/AuNPs) to other processes using the polymers inherent properties. Knowledge of the polymer as an

ionophore and polymer subunits that do not interact with the AuNPs, we can use these P4VP/AuNPs to capture metal ions from solution and then be used in a similar manner to IMAC resin beads.

In this study, the application of metal ion coordinated P4VP/AuNPs (MC/P4VP/AuNPs) to capture phosphorylated peptides and proteins, is evaluated as a tool for phospho-proteomic studies. The synthesis of P4VP/AuNPs is a simple one pot synthesis that proves stable and size controlled AuNPs, affording a platform that is simple to tailor toward a specific problem. This method is advantageous to previously described nanoparticle based phospho-peptide/protein pull down experiments[27,40,95,103,104] because there is no need for further modification of the P4VP/AuNPs prior to metal ion loading on the surface using the polymers chemical characteristics. Once the metal ions have been coordinated to the surface of the P4VP/AuNPs creating at MC/P4VP/AuNP complex, the loading of phospho-peptides/proteins is simple and allows for multiple experiments to be conducted in parallel. Since MC/P4VP/AuNPs is a solution based method for the selective capture of phospho-peptides/proteins, there is no need for the elution steps that are typically required when using column based separation techniques[37,105], making this MC/P4VP/AuNP platform for phospho-proteomics useful in both bottom-up and top-down approaches. The method demonstrates a bottom up approach proved useful in capturing phospho-peptides in standard tryptic digest solutions for both α and β casein. The MC/P4VP/AuNPs are also demonstrated capturing a whole phospho-protein (α casein) wherein the protein is this subjected to standard tryptic digest verifying the ability of the platform to also function in a top-down approach to phosphoproteomics.

Experimental

Materials

Hydrogen tetrachloroaurate (III) ($HAuCl_4$), poly(4-vinylpyridine) (P4VP), trifluoroacetic acid (TFA), methanol (MeOH), hydrogen peroxide (H_2O_2), formic acid (FA), phosphoric acid (H_3PO_4), α-casein, ammonium bicarbonate (NH_4HCO_3), 2,5-dihydroxybenzoic acid (DHB), zinc(II) chloride ($ZnCl_2$), and iron(III) chloride ($FeCl_3$) were purchased from Sigma Aldrich (St. Louis, MO). Sodium borohydride ($NaBH_4$) was purchased from EMD Chemicals Inc. (Darmstadt, Germany). Carbon coated copper 400 mesh grids were purchased from Ted Pella Inc. (Redding, CA). The peptides angiotensin I (DRVYIHPFHL), human ACTH clip 18-39 (RPVKVYPNGAEDESAEAFPLEF), bradykinin (RPPGFSPFR), bradykinin 2-9 (PPGFSPFR), and substance P (RPKPQQFFGLM-NH_2) were purchased from American Peptide Company Inc. (Sunnyvale, CA). Phosphopeptides pp60 (v-SRC) autophosphorylation site (RRLIEDNEpYTARG), and Aquaporin-2 (254-267) (RQpSVELHSPQSLPR) were purchased from AnaSpec Inc. (Fremont, CA). Molecular weight cutoff filters (MWCO) 100 kDa and 10 kDa as well as Milli-Q water were obtained from Millipore Corp. (Bedford, MA). All reagents and peptides were used as received without further purification.

Preparation of Metal Ion Coordinated/P4VP/AuNP

Gold nanoparticles (AuNPs) were synthesized using the method previously published by Hao et al.[61]. Following synthesis and ripening, the P4VP encapsulated AuNPs were lyophilized to dryness to remove the solvent. The remaining solid pellets were washed twice using 500 µL of 18 MΩ water and resuspended in 0.1% TFA, followed by sonication until the pellet was resuspended in solution. The resulting solution was further purified using MWCO filters of 100 kDa, and the solution volume was reduced to one tenth the initial volume in 0.1% TFA following purification.

Coordination of metal ions to the surface of the P4VP encapsulated AuNPs was accomplished by first diluting the purified AuNP solution to its initial volume in 0.1% TFA. The AuNP solution was then mixed 1:1 with either 200 mM $FeCl_3$ or 200 mM $ZnCl_2$, and the mixture is incubated for 30 minutes. Clean up of the metal ion coordinated P4VP/AuNPs (MC/P4VP/AuNP) was carried out by centrifugation three times using 18 MΩ and 10 kDa MWCO filters. The resulting solution of MC/P4VP/AuNPs was then used for phosphopeptide capture.

Standard Phosphopeptide Capture and Controls

The method of oxoacid modified peptide capture using MC/P4VP/AuNPs involves several steps. First, a 10 µL solution phosphopeptide was mixed with 50 µL of MC/P4VP/AuNPs. The solutions of phosphopeptides used for the capture experiments were 100 µM pp60 (v-src) autophosphorylation site and a mixture of phosphopeptides and nonphosphopeptides (bradykinin, bradykinin 2-9, angiotensin I, substance P, human

ACTH clip (18-39), aquaporin-2 (254-267), and pp60 (v-src) autophosphorylation site) each of which was present at a concentration of 100 µM. After 30 minutes of incubation, the mixture of peptides and AuNPs are centrifuged using 10 kDa MWCO filter after this washing was carried out with 18 MΩ water. The 25 µL of remaining solution was used spotting for MALDI-MS. Capture of phospho-peptides from α-casein digest was carried out as described above following α casein digest using trypsin.

The control experiment wherein aquaporin-2 (254-267) is dephosphorylated was carried out in a similar manner to the above described procedure for regular phospho-peptide capture experiments. The dephosphorylation step was carried out using standard protocol with barium hydroxide ($Ba(OH)_2$ followed by zip tipping to remove any acid or $Ba(OH)_2$ (ref). The control wherein the strength of the binding was examined was carried out using a 1:1 mixture of pp60 (v-src) autophosphorylation site and human ACTH clip 18-39 at 100 µM. The capture was carried out similarly to the process described above. However, following the wash step 2 µL of the remaining AuNP solution was mixed with DHB 1:1 and spotted for MALDI-MS analysis. This step was carried out two more times equaling three washing steps.

Whole Phosphoprotein Capture and Digest

Whole α casein was also captured using the Fe^{3+}/P4VP/AuNPs, this was carried out similarly to the phosphopeptide capture wherein 10 µL of protein solution (~10 ng) was incubated with 50 µL Fe^{3+}/P4VP/AuNPs for ~30 minutes then the mixture was washed using 100kDa MWCO filters and dH_2O. Following this capture the protein

Fe^{3+}/P4VP/AuNP complex was submitted to standard trypsin digest protocols[106]. Briefly, the protein was denatured at 90 °C for 30 minutes then cooled for ~5 minutes; trypsin was then added and the digest solution was incubated at 37 °C overnight to allow for completion of the digest. The following day the digest solution was mixed with matrix for MALDI-MS analysis. The digest of α casein in solution was carried out in using the same standard tryptic digest protocols[106].

Preparation for LDI-MS and MALDI-MS

MALDI-MS of phosphopeptides captured using MC/P4VP/AuNPs was carried out by mixing the resulting solution from the capture 1:1 with DHB. One microliter of the resulting mixture was then spotted onto a stainless steel MALDI plate and the spots were dried under vacuum. Samples of standard phosphopeptide capture were analyzed in positive mode using a Voyager - DE STR (Applied Biosystems, Framingham, MA), and samples of phospho-peptides captured from α casein digest were analyzed in positive mode with an ABI 4700 TOF-TOF (AB Sciex, Framingham, MA). The whole protein capture digest solution and the α casein solution digest were mixed 1:1 with DHB matrix, then 1 μL of this mixture was spotted onto a sample plate and vacuumed dried the resulting spots were analyzed by using an ABI 4800 MALDI TOF/TOF (AB Sciex, Framingham, MA).

Characterization of P4VP/AuNPs

Metal binding to P4VP/AuNPs was characterized using several independent methods (**Scheme 3**). UV-Vis spectroscopy (Agilent 8453, Agilent Technologies, Santa Clara, CA) was used to characterize the optical properties of the AuNPs before and after metal ions (Fe^{3+}) were bound to the surface (**Figure 6**). The spectra representing the AuNPs without metal ions bound shows a broad peak centered at ~520 nm, which suggests a broad size distribution of around 5 nm. The signal at ~250 nm corresponds to the pyridine subunits of the P4VP polymer. The UV-Vis spectrum (blue trace) resulting from the metal ion capture displays the same two main peaks at ~520 nm and ~250 nm. The peak at ~520 nm corresponding to the SPR of the AuNPs has become narrow; suggesting the size of the AuNPs following the Fe^{3+} capture has become more uniform.

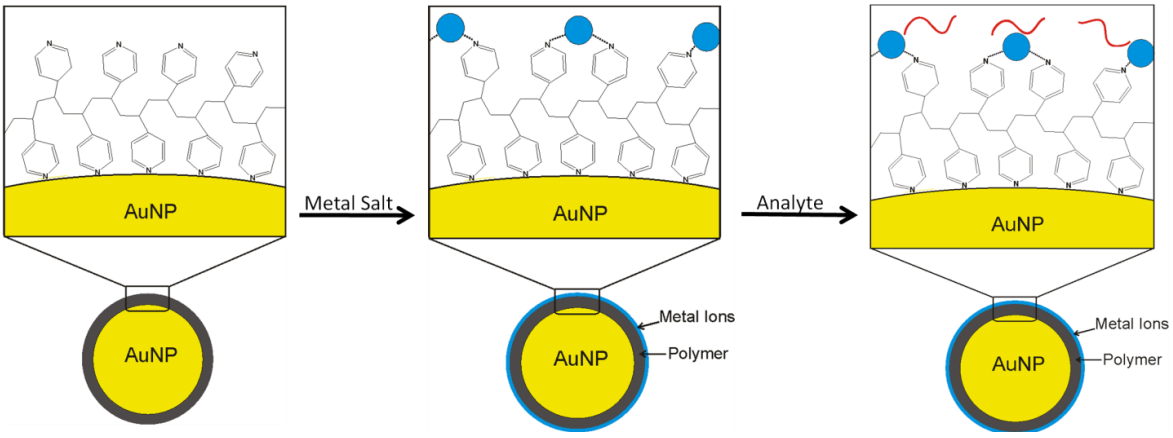

Scheme 3. A schematic representation of metal ion addition to the P4VP encapsulated AuNPs followed by the capture of specific analytes by coordination through the metal ions.

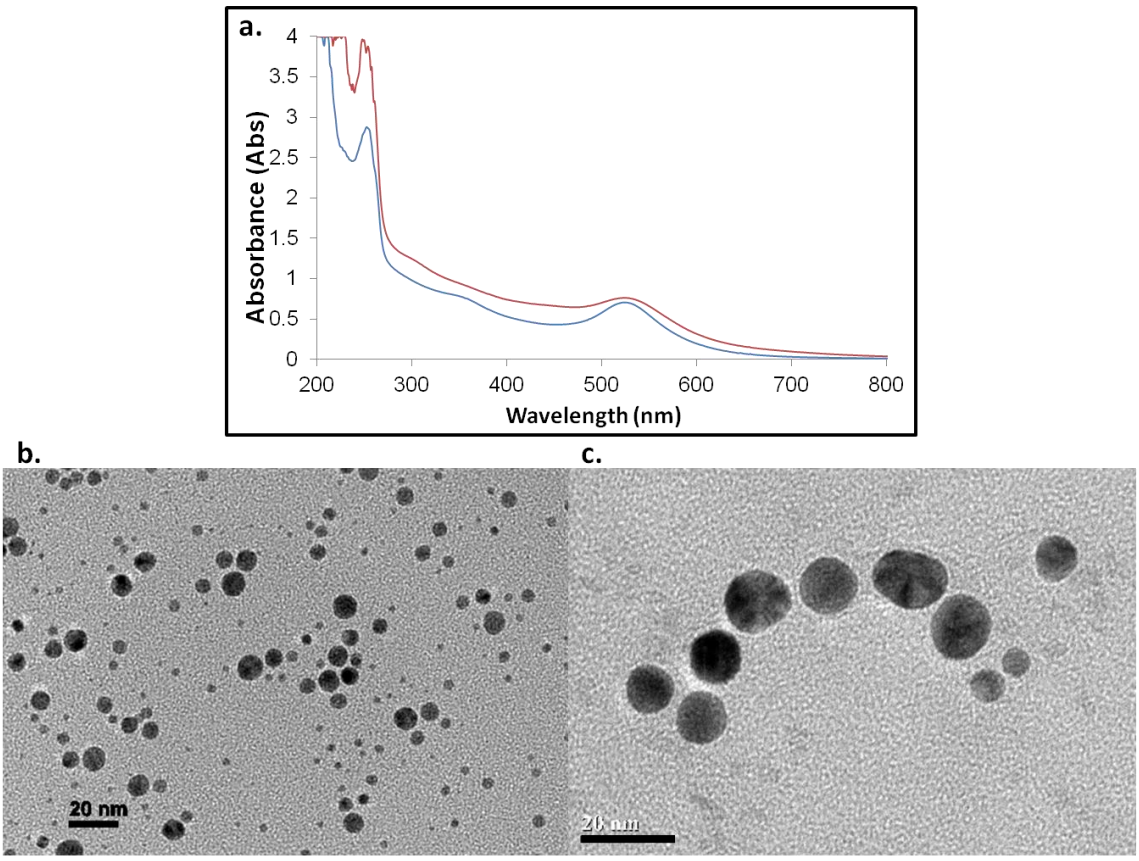

Figure 6. a. UV-Vis comparison of P4VP encapsulated AuNPs before (red) and after (blue) incubation with $FeCl_3$. b. TEM image of P4VP encapsulated AuNPs before $FeCl_3$ incubation at 100x magnification. c. TEM image of P4VP encapsulated AuNPs after $FeCl_3$ incubation at 200x magnification. The size distribution of the AuNPs before $FeCl_3$ incubation is (b) 5.0 $\pm$ 2.2 nm, and after $FeCl_3$ incubation (c) is 10.6 $\pm$ 2.8 nm. Both TEM images have 20 nm scale bars.

TEM (JEM-1200 EX, JEOL, Peabody, MA) was used to confirm the size of the P4VP encapsulated AuNPs size before and after Fe^{3+} capture (**Figure 7b** and **Figure 7c**). There is a large size distribution of AuNPs (~5.0 ± 2.2 nm) consistent with the broad peak in the UV-Vis spectrum at ~520 nm **(Figure 7b**). Addition of Fe^{3+} (as $FeCl_3$) yields a more uniform distribution of AuNP (~10.6 ± 2.8 nm) and the size distribution narrowing

corresponds to the narrow peak seen in the UV-Vis spectrum at ~520 nm (**Figure 6c**). The AuNPs' change in size can be attributed to the AuNPs being etched by the chloride ions that dissociate from the $FeCl_3$ solution used to supply the Fe^{3+} for the capture[67]. Etching of the AuNPs by the chloride ions could accelerate the process of Ostwald ripening to a time scale of ~30 minutes, which is the amount of time the AuNPs are in the $FeCl_3$ solution before the capture cleaned up as described previously (see methods).

The final characterization of the MC/P4VP/AuNPs was carried out using energy dispersive x-ray spectroscopy (EDX). This was achieved by a comparison where a carbon coated TEM grid spotted with P4VP/AuNPs and another carbon coated TEM grid was spotted with MC/P4VP/AuNPs. The EDX analysis was performed using a Tecnai G2 F20 ST FE-TEM (FEI, Hillsboro, OR) equipped with an EDX analyzer. The EDX spectrum of the P4VP/AuNPs before metal ion capture is shown in **Figure 7**. In this spectrum, the emission lines of Cu and Au are dominant. However, the spectra obtained from P4VP encapsulated AuNPs with Fe^{3+} bound the Cu and Au emission lines are still present, but there are Fe and Cl emission lines also prevalent in the lower energy range < 5 keV **(Figure 8)**. These spectral lines confirm that following the incubation of the P4VP encapsulated AuNPs with the $FeCl_3$, there is indeed Fe^{3+} captured on the surface. The growth of the chloride peak in the EDS spectrum can be explained as a ligand for the iron ions that are bound to the polymer on the surface of the AuNPs.

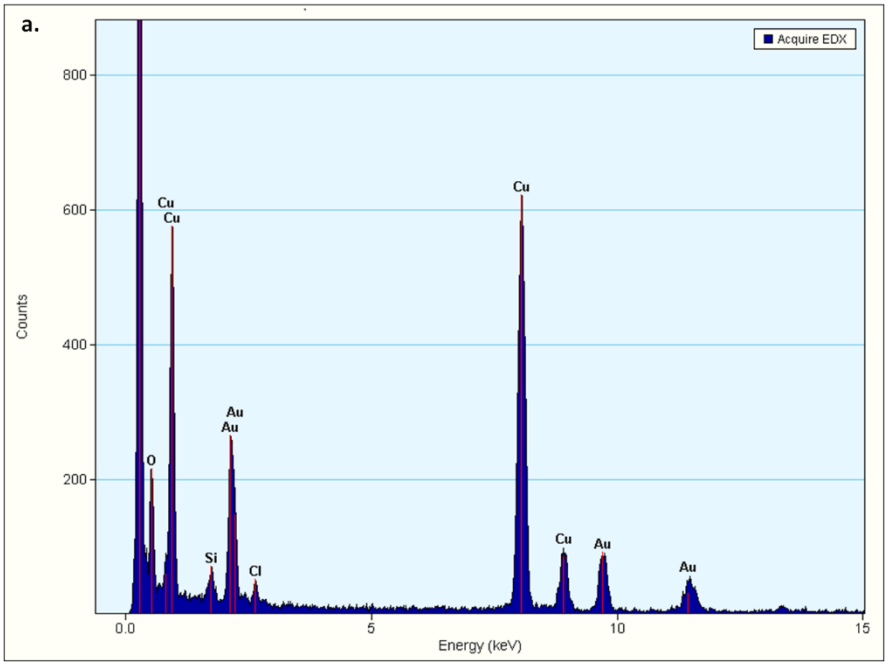

Figure 7. EDX spectrum of P4VP encapsulated AuNPs before capture of Fe^{3+}

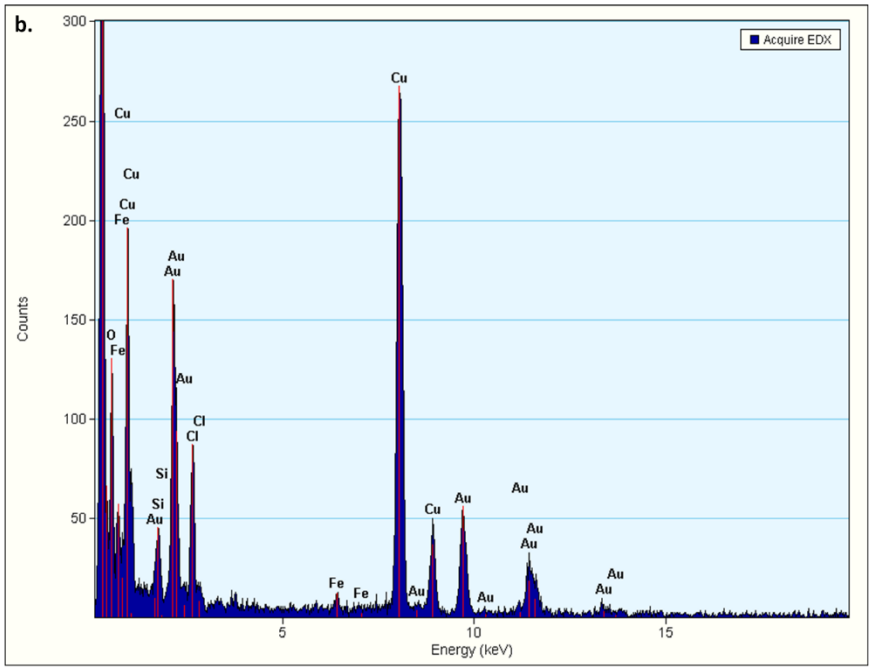

Figure 8. EDX spectrum of P4VP encapsulated AuNPs after capture of Fe^{3+}.

Results/Discussion

MC/ P4VP/AuNP are used for selective capture of oxoacid modified analytes as illustrated in **Scheme 3**. The P4VP encapsulated AuNPs were treated with metal ions, specifically Fe^{3+} and Zn^{2+}, that have demonstrated a strong affinity for oxoacid modified peptides[107,108]. These MC/P4VP/AuNPs are then are used to selectively capture phosphorylated peptides from both standard mixtures and protein digests, for use in bottom-up proteomics in a manner similar to traditional immobilized metal affinity chromatography (IMAC). We also demonstrate the use of MC/P4VP/AuNPs to capture whole proteins and digest the proteins while captured on the surface allowing for top-down proteomics.

The ability of the MC/P4VP/AuNPs to capture oxoacid modified peptides was examined using pp60 (v-src) autophosphorylation site (m/z 1672.2, RRLIEDNEpYTARG). First, the Fe^{3+}/P4VP/AuNPs were used to capture pp60 (v-src) autophosphorylation site at a concentration of 100 µM from water as described in the experimental section. When using Fe^{3+}/P4VP/AuNPs to capture oxoacid modified peptides, the addition of matrix is required due to the lack of a protonation source within the system. The lack of protonation is an effect of Fe^{3+} ions binding to the surface of the P4VP AuNPs through the pyridyl nitrogens. The matrix used throughout the entire study when analyzing phosphopeptide capture was 2,5-dihydroxybenzoic acid, which has been reported to assist in the ionization of phosphorylated peptides[109]. The mass spectrum obtained using methods described in the experimental section shows the protonated signal for the phosphorylated peptide **(Figure 9**). It also contains several peaks that are associated

with the pp60 (v-src) autophosphorylation site sample. The results of the pp60 provided proof-of-concept that Fe^{3+}/P4VP/AuNPs efficiently captures phosphopeptides out of water. These data control experiments are necessary to characterize the effects of the P4VP polymer and the Fe^{3+} might have on the capture of the phospho-peptides when using Fe^{3+}/P4VP/AuNPs.

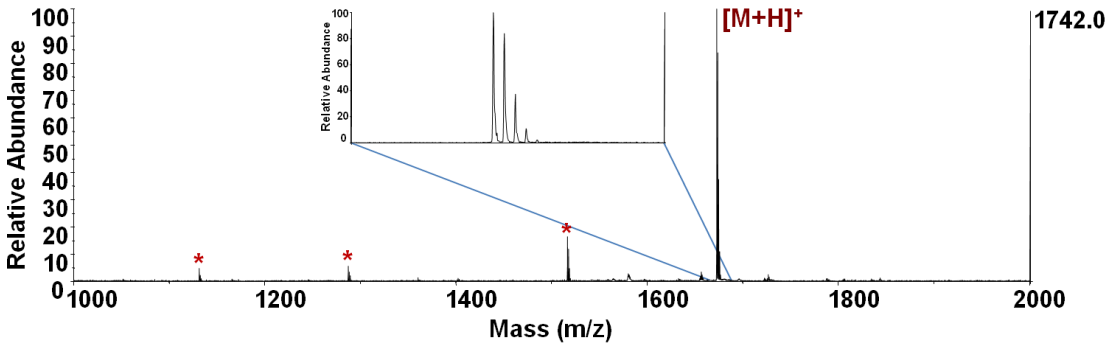

Figure 9. a. MALDI mass spectrum of 100µM pp60 (v-src) autophosphorylation site (m/z 1672.2, RRLIEDNEpYTARG) after being captured. The * labeled peaks are contaminants from the peptide and/or the matrix used for analysis.

Several control experiments were performed to determine if the Fe^{3+} formed a metal oxide layer on the surface of the AuNPs or if the P4VP is capturing the Fe^{3+} ions. The control was carried out by incubating the $FeCl_3$ with citrate capped AuNPs, and the phosphopeptide capture experiment using pp60 (v-src) autophosphorylation site in water was performed. The resulting solution was analyzed with by MALDI-MS (see experimental section). The mass spectrum did not contain any signals for the pp60 autophosphorylation site, suggesting there were no metal ions present at the surface to facilitate the capture of the phosphate group attached to the peptide. The absence of

analyte signal highlights the need for the P4VP on the surface of the AuNPs; this absence also suggests there are pyridine groups that are not bound to the surface of the AuNPs that can bind the metal ions, specifically in this case, Fe^{3+} from a solution of $FeCl_3$.

A second control was performed to determine if the Fe^{3+} ions are an important factor in the capture of the phospho-peptide. This control experiment was accomplished by incubating pp60 (v-src) autophosphorylation site with P4VP/AuNPs without Fe^{3+} ions present in the solution. The mass spectra from this sample show no evidence for phosphopeptide capture, **Figure 10**. Therefore, these two control experiments provide evidence that the polymer P4VP is important in capturing the Fe^{3+}, yet plays no significant role in capturing the phospho-peptide from solution. The capture of the phosphopeptide is facilitated not by the P4VP but by the Fe^{3+} ions coordinated to the P4VP polymer on the AuNP surface. The Fe^{3+} ions are coordinated to the P4VP and do not form a metal oxide layer on the AuNPs surface. These findings demonstrate the importance of the P4VP being in the Fe^{3+}/P4VP/AuNP system as a surface modification for the AuNPs, in preventing the Fe^{3+} ions to form a core shell structure with the AuNPs, yet allowing for Fe^{3+} ion coordination in a manner that is accessible to phosphate group which is the PTM found for this peptide.

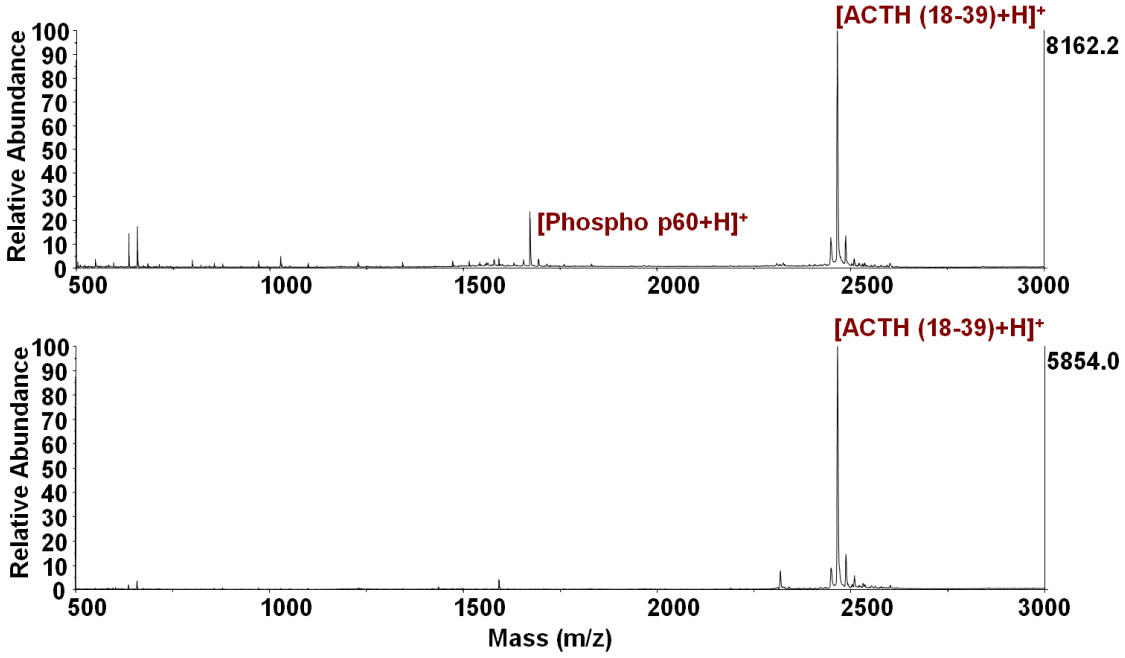

Figure 10. a. MALDI-MS spectra of a mixture of 1:1 of 100 µM pp60 (v-src) autophosphorylation site (m/z 1672.2, RRLIEDNEpYTARG) and human ACTH clip 18-39 (m/z 2465.7, RPVKVYPNGAEDESAEAFPLEF). b. MALDI-MS spectra of the above mixture following the capture experiement using P4VP/AuNPs without metal ions bound.

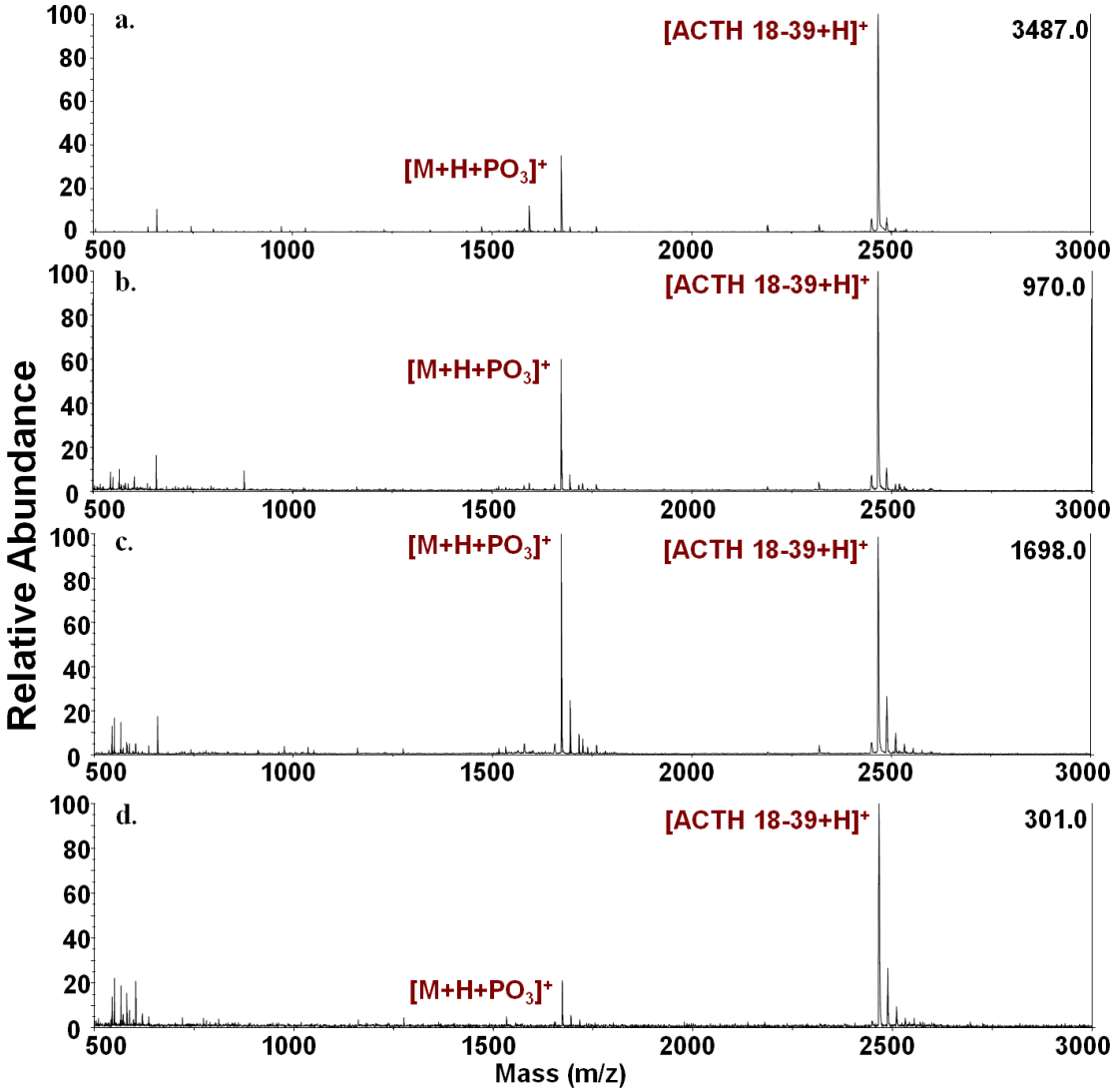

Figure 11. a. MALDI-MS spectra of a mixture of 1:1 of 100 µM pp60 (v-src) autophosphorylation site (m/z 1672.2, RRLIEDNEpYTARG) and human ACTH clip 18-39 (m/z 2465.7, RPVKVYPNGAEDESAEAFPLEF). b. MALDI-MS spectra of the above mixture following the capture experiment using Fe^{3+}/P4VP/AuNPs following the first watch step. c. MALDI-MS spectra of the mixture following the capture experiment using Fe^{3+}/P4VP/AuNPs following the second wash step. d. MALDI-MS spectra of the mixture following the capture experiment using Fe^{3+}/P4VP/AuNPs following the third wash step.

Finally, as a control, we wanted to determine the robustness of the MC/P4VP/AuNP phosphopeptide capturing method to withstand several washing steps. This study was accomplished using a mixture 1:1 of pp60 (v-src) autophosphorylation site and human ACTH clip 18-39. The results of this control, **Figure 11**, demonstrate the ability of this method to bind phosphopeptides strongly enough to withstand several washing cycles. Though the peptide signal for the phosphopeptide decreases significantly in the third washing step the signal is still present and sufficient for making an accurate assignment of the peptide. Also from this mixture, peptide ACTH 18-39 (RPVKVYPNGAEDESAEAFPLEF m/z = 2456.7 pI = 4.25) is retained after the phosphopeptide capture. Human ACTH 18-39 is an acidic peptide which led to peptide retention throughout the phosphopeptide capture process through hydrogen bonding interactions similarly to the original manuscript published by Hao et al[61]. The retention of acidic peptides is also known to occur in traditional IMAC columns also[88,110].

The capture experiment used to simulate a complex system, such as a digest, involved a mixture of peptides and phosphopeptides. The mixture contained two phospho-peptides and five non-phospho-peptides (**Table 1**). The mixture of peptides was treated in the same manner as the single phosphopeptide sample. The results before and after phosphopeptide capture are shown (**Figure 12**). The spectrum before phosphopeptide capture demonstrates the phosphopeptides are present in low abundance relative to the other five nonphospho-peptides; these results are typically seen in proteomic samples with phosphorylated peptides present[111] (**Figure 12a**). The mass spectrum taken following the phosphopeptide capture illustrates this method's ability to capture phosphopeptides from the mixture and increase their relative abundance in the resulting mass spectrum **(Figure 12b**).

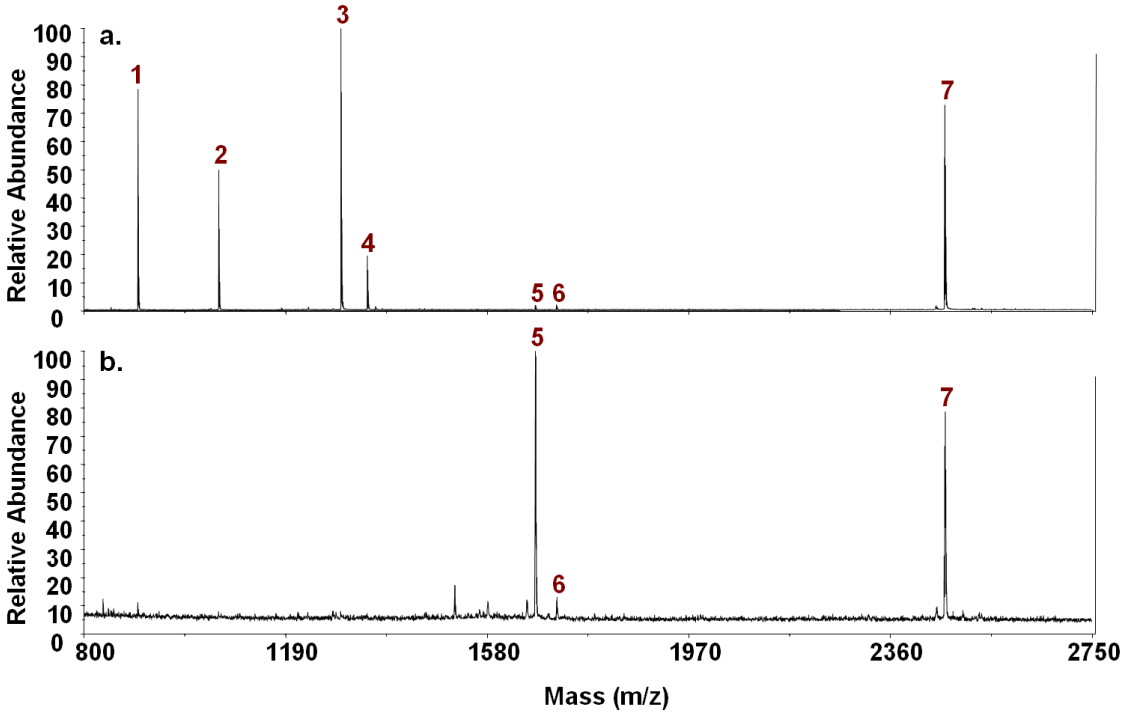

Figure 12. MALDI mass spectra of 10μM phosphorylated peptides mixed with non-phosphorylated peptides labeled (Table 1.). a. before phospho-capture and b. after phospho-capture using the Fe^{3+} ions bound to the P4VP encapsulated AuNPs.

Number	Peptide	Sequence	Molecular Weight	pI
1	Bradykinin 2-9	PPGFSPFR	904.0	10.18
2	Bradykinin	RPPGFSPFR	1060.2	12.00
3	Angiotensin I	DRVYIHPFHL	1296.5	6.92
4	Substance P	RPKPQQFFGLM-NH_2	1347.7	11.00
5	pp60(v-SRC)	RRLIEDNEpYTARG	1672.2	4.68*
6	Aquaporin-2 (254-267)	RQpSVELHSPQSLPR	1713.8	6.49*
7	ACTH (18-39)	RPVKVYPNGAEDESAEAFPLEF	2465.7	4.25

Table 1. List of numerical labels of phosphorylated peptides and non-phosphorylated peptides with sequence, molecular weight, and pI (MW and pI calculated using expasy.org; the phosphopeptide pI was calculated using scansite.mit.edu). * denotes the pI of the peptide with phosphorylation.

The sequence of the phosphopeptides used in this mixture also contains several acidic amino acids including: pp60 (v-src) autophosphorylation site (RRLIEDNEpYTARG) and Aquaporin-2 (254-267) (RQpSVELHSPQSLPR). In the original P4VP encapsulated AuNP manuscript, the pyridine subunits not bound to the surface of the AuNP were used to build up layers of AuNPs on polymers with acidic subunits through hydrogen bonding[61]. Therefore, another control experiment is necessary to determine whether the phosphate group or the acidic amino acid side chains are more important during the phospho-peptide capture experiment. For example, Aquaporin-2 was dephosphorylated (see experimental section) to produce a dehydroalanine form of the peptide (RQdhaVELHSPQSLPR). From this protocol, a mixture of both phospho- and dephosphopeptide results is seen in the MALDI-MS (**Figure 13a**). The dephosphorylated peptide is the most abundant ion seen in the mass spectrum and the phosphopeptide is ~15% of the relative abundance of the dephospho-peptide. However, when the phosphopeptide capture is performed on the mixture, the phosphopeptide becomes the most abundant ion observed in the mass spectrum (**Figure 13b)**. This experiment demonstrates the importance of the phosphate group compared to the acidic properties of the peptide when employing P4VP encapsulated AuNPs with Fe^{3+} bound to capture phospho-peptides.

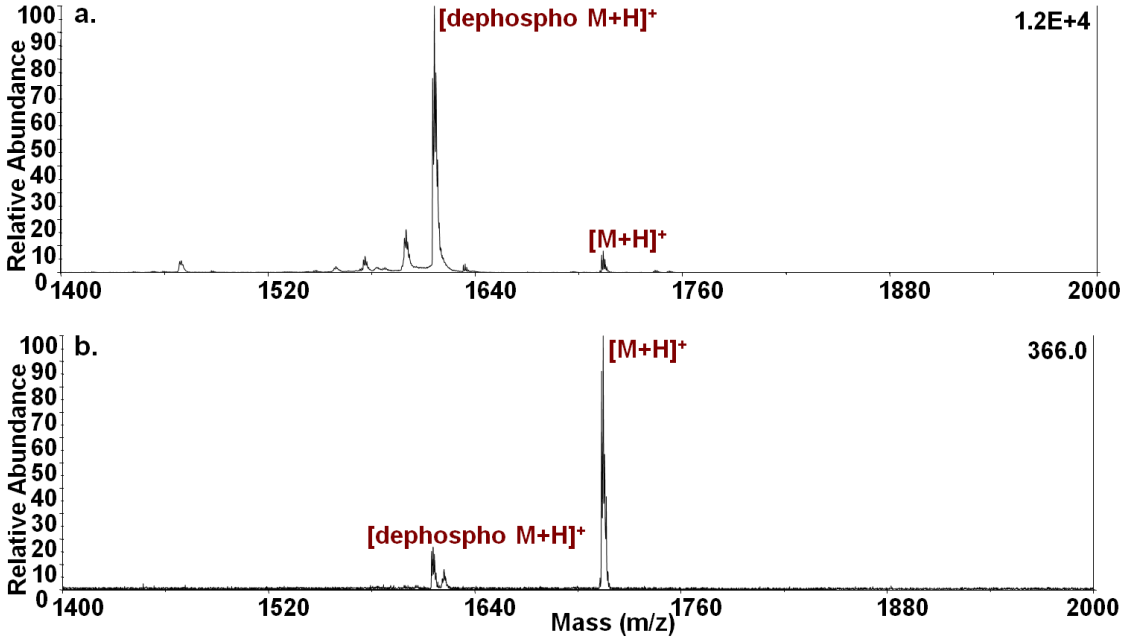

Figure 13. a. MALDI mass spectrum of 100 µM Aquaporin-2 (254-267) (m/z 1713.8, RQpSVELHSPQSLPR-OH) following dephosphorylation. B. MALDI mass spectrum of 100 µM Aquaporin-2 (254-267) (m/z 1713.8, RQpSVELHSPQSLPR-OH) following dephosphorylation and phosphor-capture using Fe^{3+} ion bound to P4VP encapsulated AuNPs.

The general utility of Fe^{3+}/P4VP/AuNPs for application as a bottom-up phosphoproteomic tool was evaluated using a tryptic digest of the phosphoprotein, α and β casein. α casein digest was analyzed before and after the phospho-peptide capture was performed using MALDI-MS with DHB, **(Figure 14a** and **Figure 14b**). The mass spectrum contains two peaks (labeled with asterisk) at m/z 1951.95 (YKVPQLEIVPNpSAEER) and m/z 1660.79 (VPQLEIVPNpSAEER), that correspond to phosphorylated peptides from the α-casein digest. These two peptides are similar peptides; the m/z 1951.95 peptide is the result of a missed tryptic cleavage at the lysine in position two for the m/z 1951.95 (YKVPQLEIVPNpSAEER), which would result in the

m/z 1660.79 peptide. There are dashed lines that run through the phosphorylated peptide peaks for all three spectra (**Figure 14**). In the mass spectrum of the digest prior to the phospho-peptide capture, the dashed lines represent two phospho-peptide peaks, which are not visible above the base line of the spectrum **(Figure 14a**). The phospho-peptide capture performed using Fe^{3+}/P4VP/AuNPs display an increase in relative abundance of the phospho-peptides when compared to the nonphospho-peptides (**Figure 14b**). In addition to iron, multiple other metal ions have been shown to work in traditional IMAC columns, including Zn and Ga[107,112]. Since P4VP is a polymer that is used to bind metal ions, Zn^{2+} was used for phospho-peptide capture in place of Fe^{3+} [82]. The results of the phosphopeptide capture of α-casein digest using zinc (II) can be seen in **Figure 14c**. The mass spectrum has the two peaks associated with the phospho-peptides m/z 1951.95 and m/z 1660.79 (**Figure 14c**).

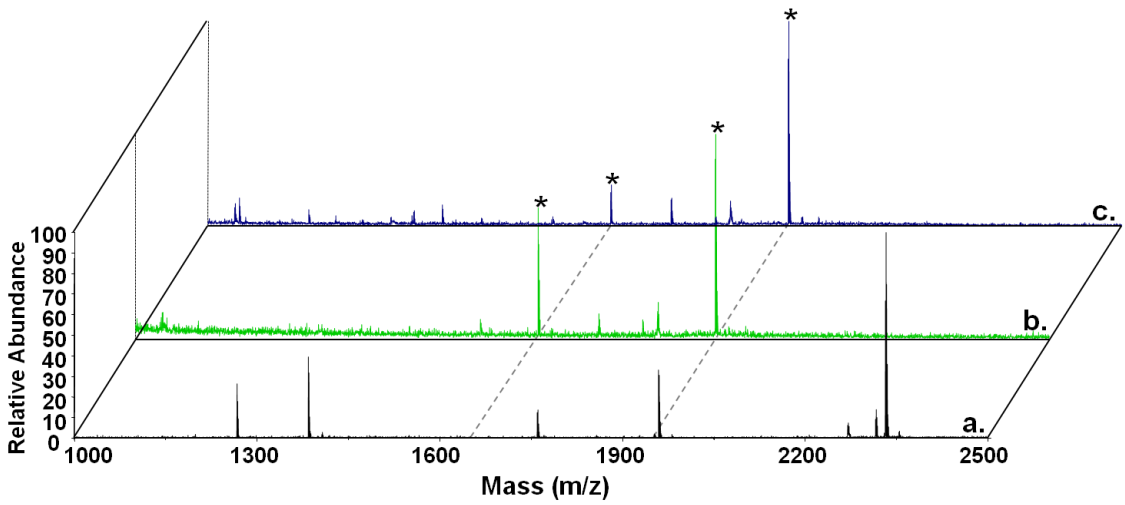

Figure 14. MALDI Mass spectra of α casein a. Full digest before phosphopeptide enrichment. b. Phosphopeptide enrichment using Zn (II) ions bound to P4VP AuNPs, and c. phosphopeptide enrichment using Fe (III) ions bound to P4VP AuNPs. * indicates phosphopeptides corresponding to m/z 1951.95 (YKVPQPLEIVPNpSAEER) and m/z 1660.79 (VPQLEIVPNpSAEER).

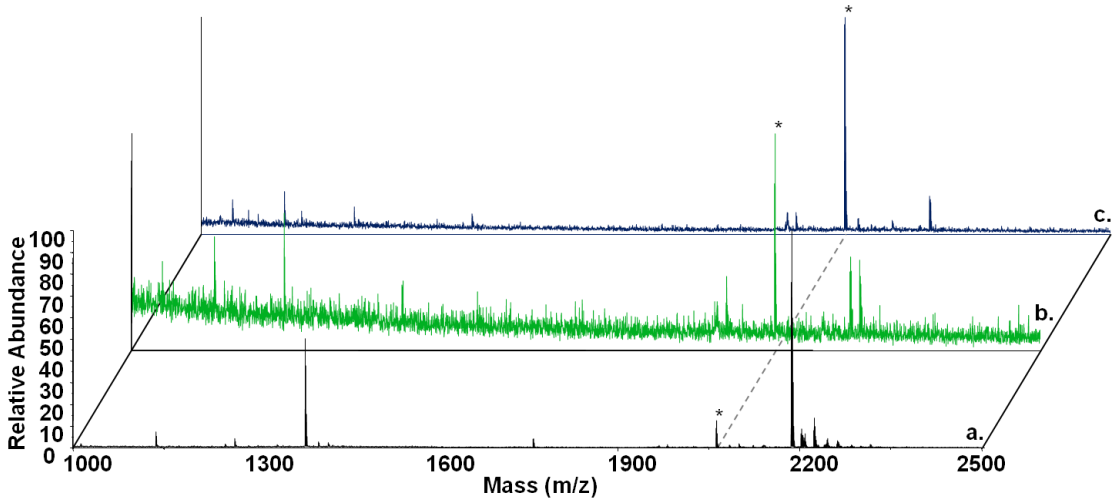

Figure 15. MALDI mass spectra of β casein. a. full digest of β casein before phosphopeptides enrichment. b. Phosphopeptide enrichment using Zn (II) ions bound to P4VP AuNPs. * indicates phosphopeptides corresponding to m/z 2061.97 (FQpSEEQQQTEDELGDK). c. Phosphopeptide enrichment using Fe (III) ions bound to P4VP AuNPs. * indicates phosphopeptides corresponding to m/z 2061.97 (FQpSEEQQQTEDELGDK)

These data demonstrate this method of phospho-peptide capture is not limited to just using Fe^{3+} as the metal ion used for phospho-peptide capture. The data for β casein **Figure 15**, further demonstrates this methods ability to capture phospho peptides from a phospho protein digest using Fe^{3+} and Zn^{2+} through the retention of m/z 2061.97 (FQpSEEQQQTEDELGDK) following capture. The data also demonstrates that using P4VP encapsulated AuNPs with metal ions bound at the surface have the ability to work in proteomic environments that are traditionally encountered in today's research laboratories.

The use of the Fe^{3+}/P4VP/AuNPs as a top-down phosphoproteomic tool was evaluated by submitting a whole phosphoprotein (α casein) to capture and digest on the surface of the AuNP complex with no need for elution or special handling steps. The capture was carried out similarly to the capture of phosphopeptides described above, where 10 µL of protein was mixed with 50 µL of Fe^{3+}/P4VP/AuNP. The protein at 10 µg was captured and digested off the surface with no elution of the protein, resulting in the spectra **Figure 16a**.

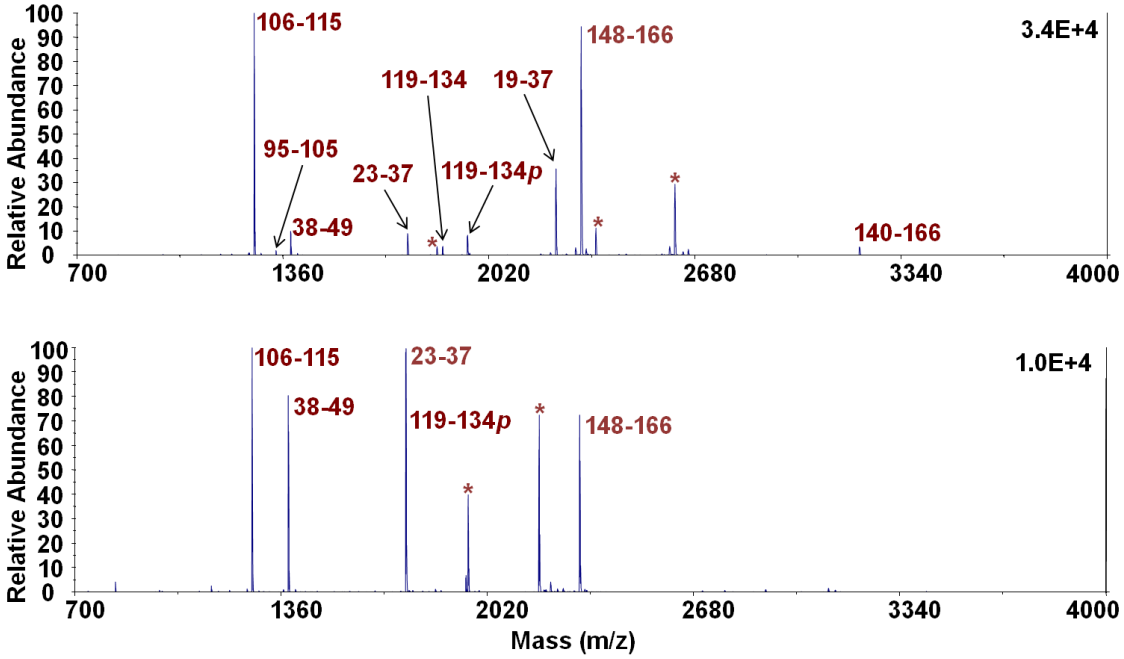

Figure 16. Top, MALDI mass spectra of α casein (~10 ng) digested using trypsin. Bottom, MALDI mass spectra of α casein after capture using Fe3+/P4VP/AuNPs and digested with trypsin. All peptides are labeled using their corresponding residue numbers. * indicated peptides not associated with α casein digest fragments. p indicated peptides that correspond to phosphorylated peptides.

Seen in this spectrum are peaks that correspond to 9 peptides from the digest of the protein. Of these peptides, there is one peptide present that is a known phosphopeptide at m/z 1951.95 (119-134, YKVPQLEIVPNpSAEER). This being the only phosphopeptide present in the spectrum is not cause for concern, as the non-phosphopeptides were not removed from the sample prior to analysis, to demonstrate the ability of the Fe^{+}/P4VP/AuNPs to capture whole proteins and allow for on particle digestion of the protein. This data provides evidence for the ability to digest the protein still on the particles, also when comparing the on particle digest to the protein digested from solution

(**Figure 16b**) there are significantly more peptides present that correspond to the sequence of α casein (**Table 2**).

Conclusion

The capture of phosphorylated peptides using poly (4-vinylpyridine) (P4VP) encapsulated AuNPs with metal ions bound to the surface is reported using mass spectrometry. The P4VP encapsulated AuNPs were characterized before and after metal ion capture in order to determine the physical and/or optical changes the AuNPs might undergo. The method was accomplished and demonstrated using Fe^{3+} captured on the surface of the AuNPs during the incubation step. It was also determined that after Fe^{3+} was captured on the surface of the AuNPs, the size of the particles became larger and the distribution of the sizes became narrower. Changes in the size distribution is an effect of Ostwald ripening that is hastened by halide ion etching of the AuNPs during the $FeCl_3$ incubation step[67]. Following characterization of the physical and optical properties of the AuNPs, the AuNPs were used to capture phospho-peptides from mixtures and digest. We first demonstrated the Fe^{3+}/P4VP/AuNPs were able to capture phosphorylated peptides, using a single phospho-peptide pp60 (v-src) autophosphorylation site (RRLIEDNEpYTARG). With this peptide, we were able to show the P4VP encapsulated AuNPs with metal ions bound are able to capture the phospho-peptide out of water. Although the capture is possible using the AuNPs, we had to use a traditional MALDI matrix, DHB, because there is no protonation source available on the AuNPs with the metal ions and phospho-peptide bound. Using the AuNPs as the phospho-peptide capture

"beads" in solution means there are fewer sample handling steps when compared to traditional phosphopeptide capture techniques.

Fragment Mass (m/z)	Fragment Residue Position	Modifications	Modified Fragment Mass	Fragment Sequence
7013.292	148-208			EPMIGVNQELAYFYPELFRQFYQLDAYPSGAWYYVPLGTQYTDAPSFSDIPNPIGSENSEK
5445.525	167-214			QFYQLDAYPSGAWYYVPLGTQYTDAPSFSDIPNPIGSENSEKTTMPLW
4716.173	167-208			QFYQLDAYPSGAWYYVPLGTQYTDAPSFSDIPNPIGSENSEK
4069.822	58-94	Phos: 61, 63,79,81,82,83,90	4629.587	DIGSESTEDQAMEDIKQMEAESISSSEEIVPNSVEQK
3207.593	140-166			EGIHAQQKEPMIGVNQELAYFYPELFR
3125.657	23-49			HQGLPQEVLNENLLRFFVAPFPEVFGK
2827.378	74-98	Phos: 79, 81,82,83,90	3227.209	QMEAESISSSEEIVPNSVEQKHIQK
2438.124	52-73	Phos: 56, 61,63	2678.023	VNELSKDIGSESTEDQAMEDIK
2321.081	74-94	Phos: 79, 81,82,83,90	2720.913	QMEAESISSSEEIVPNSVEQK
2316.137	148-166			EPMIGVNQELAYFYPELFR
2235.236	19-37			HPIKHQGLPQEVLNENLLR
2177.138	121-139	Phos: 130	2257.105	VPQLEIVPNSAEERLHSMK
2080.071	99-115			EDVPSERYLGYLEQLLR
1871.986	119-134	Phos: 130	1951.952	YKVPQLEIVPNSAEER
1767.759	58-73	Phos: 61, 63	1927.692	DIGSESTEDQAMEDIK
1759.945	23-37			HQGLPQEVLNENLLR
1641.868	38-51			FFVAPFPEVFGKEK
1580.828	121-134	Phos: 130	1660.794	VPQLEIVPNSAEER
1508.884	106-117			YLGYLEQLLRLK
1506.785	135-147			LHSMKEGIHAQQK
1384.73	38-49			FFVAPFPEVFGK
1337.681	95-105			HIQKEDVPSER
1267.705	106-115			YLGYLEQLLR
946.5204	50-57	Phos: 56	1026.487	EKVNELSK
910.4741	140-147			EGIHAQQK
875.5573	16-22			RPKHPIK
831.3843	99-105			EDVPSER
748.3698	209-214			TTMPLW
689.3828	52-57	Phos: 56	769.3491	VNELSK

Table 2. List of peptide fragments with molecular weight, fragment residues, modifications, modified fragment molecular weight, and sequence from an α casein digest using trypsin (information was determined using expasy.org/peptide_mass/).

The use of these MC/P4VP/AuNPs to capture phospho-peptides from a protein digest was also accomplished using two traditional IMAC metal ions, Fe^{3+} and Zn^{2+}. The ability to capture phospho-peptides from a protein digest using two different metal ions demonstrates the robustness of this method and the applicability of these AuNPs in

traditional phosphoproteomic studies in a bottom up approach. This method also proves useful as a tool for whole protein capture and digests which allows for more applications in phosphoproteomic studies as a top-down technique.

CHAPTER IV

CYSTEIC ACID MODIFIED PEPTIDE ENRICHMENT USING POLY(4-VINYLPYRIDINE) COATED GOLD NANOPARTICLES

Introduction

Amino acid side chains play important roles in protein function making up active sites for enzymatic function and influencing protein structure[113]. The side chains of amino acid control the function and structure of proteins through various modifications known as post translational modifications (PTMs) [64]. TMs vary from the addition of alkyl chains to reversible phosphorylation [113]. One PTM of interest is the oxidation of cysteine and methionine side chain thiols. The oxidation of these thiols is important for cellular processing of reactive oxygen species (ROS) and reactive nitrogen species (RNS) [114,115]. In the case of cysteine there are three possible oxidation states sulfenic acid (R-SOH), sulfinic acid ($R\text{-}SO_2H$), and sulfonic acid ($R\text{-}SO_3H$) [116,117]. Sulfenic and sulfinic acid are oxidation of the thiol with one and two oxygen's respectively. These two oxidation states are reversible and are the major pathways for processing of ROS/RNS. Sulfonic acid modified cysteine also known as cysteic acid is the direct product of oxidative stress and is irreversible [118,119].

The study of cysteine oxidation is important and the determination of oxidation sites has been studied using several methods. Reactive cysteines have been profiled using isotope-coded affinity tagging (ICAT), attaching the tags to cysteines using thiol reactive agents [120]. This ICAT method allows for the profiling of reactive cysteines within proteins

because the ICAT labeling agent will only interact with thiols that have not been oxidized [120]. While using this method is effective at determining the reactive cysteine sites within proteins, it lacks in ability to determine the oxidation state of the unlabeled thiols [121]. This is a major drawback when trying to determine the oxidation products of cysteine present proteins due to the number of possible oxidation states for cysteine.

Increased interest in the oxidation of cysteine from redox process in cells has lead to the development of methods of studying cysteine oxidation that are dependent on the oxidation state of the cysteines present in the sample. Therefore, methods have been developed to study cysteine oxidation based on the oxidation states of cysteine have been developed. The first oxidation state of cysteine is sulfenic acid (R-SOH), where the thiol has undergone one step of oxidation by ROS or RNS. This oxidation state has been studied by Carroll *et al.* using dimedone to study cysteine oxidation in cells [122,115]. Dimedone is a chemical modifier that selectively targets sulfenic acid over the other oxidation states of thiol as well as unoxidized thiol [48,122,115]. The second oxidation state of cysteine is sulfenic acid ($R\text{-}SO_2H$), this product is formed as the second step in cysteine oxidation and is reversible [123]. Sulfinic acid cysteine is a quick reacting intermediate that reacts very quickly following two possible pathways **i)** further oxidation to sulfonic acid cysteine and **ii)** reduction back to the thiol or sulfenic acid cysteine [119]. This reaction intermediate is very unstable and reacts on a time scale that makes studying it very difficult [124]. The final oxidation product of cysteine is the most stable, sulfonic acid cysteine ($R\text{-}SO_3H$) [28]. Sulfonic acid cysteine is the irreversible oxidation of cysteine that can be used in determining the oxidative stress levels in cells [119]. There are a few techniques that have

been presented previously that work to elucidate sulfonic acid cysteines in peptides and proteins. First, antibodies specific for proteins that have been oxidized have been used for selective enrichment of sulfonic acid cysteine in molecular chaperone activity studies [119]. The next method is more relevant for this study because nanomaterials are the platform for enrichment. Briefly, Chang *et al.* functionalized nanodiamonds with polyarginine which electrostatically interacts with the sulfonic acid allowing for enrichment of the modified peptide [28]. This method demonstrates the ability of non-antibody and non-labeling techniques for the selective enrichment of sulfonic acid cysteine modified peptides. When the nanodiamonds technique was challenged with phospho peptides as a possible interference for the electrostatic interaction there was no phospho peptide retained, meaning the selectivity of this method is very high even in the presence of other similar oxoacid PTMs [28].

In previous studies nanomaterials have been used for PTM enrichment [52,86,125]. In this report we use a one pot synthesis of gold nanoparticles (AuNPs) that are functionalized with the polymer poly(4-vinylpyridine) (P4VP) to capture peptides containing sulfonic acid cysteines. Specifically, we use metal ions bound to the surface of the AuNPs through the polymer in a manner similar to enrichment used previously for phospho-peptides [103]. The metals chosen for this method were Fe^{3+} and Mn^{2+} which have been shown previously to interact strongly with sulfonic acid in water [116,126]. The selectivity of this method for sulfonic acid cysteine peptides over phospho-peptides is demonstrated through used of these different metal ions.

Experimental

Materials

Hydrogen tetrachloroaurate (III) ($HAuCl_4$), poly(4-vinylpyridine) (P4VP), trifluoroacetic acid (TFA), methanol (MeOH), manganese(II) chloride ($MnCl_2$), hydrogen peroxide (H_2O_2), formic acid (FA), phosphoric acid (H_3PO_4), 2,5-dihydroxybenzoic acid (DHB), α-Cyano-4-hydroxycinnamic acid (CHCA), and iron(III) chloride ($FeCl_3$) were purchased from Sigma Aldrich (St. Louis, MO). Sodium borohydride ($NaBH_4$) was purchased from EMD Chemicals Inc. (Darmstadt, Germany). Hydrogen peroxide (35% wt/wt) and formic acid (99% wt/wt) were purchased from Acros Organics (Morris Plains, NJ, USA). Carbon coated copper 400 mesh grids were purchased from Ted Pella Inc. (Redding, CA). The peptides human ACTH clip 18-39 (RPVKVYPNGAEDESAEAFPLEF) and flag (DYKDDDDK) were purchased from American Peptide Company Inc. (Sunnyvale, CA). The peptides LVINVCLSQG, CLVINLSQR, Aquaporin-2 (254-267) (RQpSVELHSPQSLPR), and pp60 (v-src) autophosphorylation site (RRLIEDNEpYTARG) were purchased from AnaSpec Inc. (Fremont, CA). Molecular weight cutoff filters (MWCO) 100 kDa and 10 kDa as well as Milli-Q water were obtained from Millipore Corp. (Bedford, MA). All reagents and peptides were used as received without further purification.

Preparation of Metal Ion Coordinated/P4VP/AuNP

Gold nanoparticles (AuNPs) were synthesized using the method previously published by Hao et al.[61]. Following synthesis and ripening, the P4VP encapsulated AuNPs were lyophilized to dryness to remove the solvent. The remaining solid pellets were washed twice using 500 µL of 18 MΩ H_2O and resuspended in 0.1% TFA, followed by sonication until the pellet was resuspended in solution. The resulting solution was further purified using MWCO filters of 100 kDa, and the solution volume was reduced to one tenth the initial volume in 0.1% TFA following purification. The size of the P4VP/AuNPs was characterized using TEM (JEM-1200 EX, JEOL, Peabody, MA).

Coordination of metal ions to the surface of the P4VP encapsulated AuNPs was accomplished by first diluting the purified AuNP solution to its initial volume in 0.1% TFA. The AuNP solution was then mixed 1:1 with either 200 mM $FeCl_3$ or 200 mM $MnCl_2$, and the mixture is incubated for 30 minutes. Clean up of the metal ion coordinated P4VP/AuNPs (MC/P4VP/AuNP) was carried out by centrifugation three times using 18 MΩ H_2O and 10 kDa MWCO filters. The resulting solution of MC/P4VP/AuNPs was then used for phosphopeptide capture.

Solution Phase Performic Oxidation

Peptides containing cysteines were oxidized using a standard oxidation method previously described producing LVINVCoxLSQG and CoxLVINLSQR [127]. Following oxidation the peptides were diluted to 500 µL using 18 MΩ H_2O and vacuumed dry.

Following this the peptides were then resuspended to 1 mg/mL and stored frozen until need for experiments.

Sulfonic Acid Cysteine Peptide Capture and Controls

The method of oxoacid modified peptide capture using MC/P4VP/AuNPs involves several steps. First, a 10 µL solution sulfonic acid cysteine peptide (cysteic acid) was mixed with 50 µL of MC/P4VP/AuNPs. The solutions of cysteic acid used for the capture experiments were 100 µM LVINVCoxLSQG and CoxLVINLSQR. A mixture of cysteic acid peptide and regular peptides were comprised of either LVINVCoxLSQG mixed 1:1 with human ACTH clip 18-39 or CoxLVINLSQR mixed 1:1 with flag, all peptides in these mixtures were at concentrations of 100 µM. After 30 minutes of incubation, the mixture of peptides and AuNPs are centrifuged using 10 kDa MWCO filter after this washing was carried out with 18 MΩ water. The 25 µL of remaining solution was used spotting for MALDI-MS. A mixture of LVINVCoxLSQG, CoxLVINLSQR, Aquaporin 2, and pp60 (v-src) autophosphorylation site at a ratio of 1:1 and a concentration of 100 µM was also made for used with the enrichment method to determine selectivity. 10 µL of this mixture was mixed with 50 µL of Mn^{2+}/P4VP/AuNPs the solution was allowed to incubate for ~30 minutes before being washed using MWCO filters. After the washing of the mixture the solution was spotted for MALDI-MS analysis.

Controls were performed using LVINVCLSQG. The peptide at 100 µM was mixed with P4VP/AuNPs and Mn^{2+}/P4VP/AuNPs and subjected to the enrichment method

using 10 kDa MWCO filter after this washing was carried out with 18 MΩ water. The resulting solutions were removed and spotted for MALDI-MS analysis.

Preparation for LDI-MS and MALDI-MS

MALDI-MS of cysteic acid peptides captured using MC/P4VP/AuNPs was carried out by mixing the resulting solution from the capture 1:1 with CHCA. One microliter of the resulting mixture was then spotted onto a stainless steel MALDI plate and the spots were dried under vacuum. Samples of standard cysteic acid peptide capture solutions were analyzed in the positive and negative mode using a Voyager - DE STR (Applied Biosystems, Framingham, MA).

Results and Discussion

Methods employing nanomaterials for enrichment of PTM has become an emerging field in proteomic research. The use of metal ion coordinated P4VP encapsulated AuNPs (MC/P4VP/AuNPs) for enrichment sulfonic acid modified cysteines (cysteic acid) is described in this report (**Scheme 4**). The use of different metal ions is demonstrates this methods ability to be applied for selective enrichment of similar PTMs.

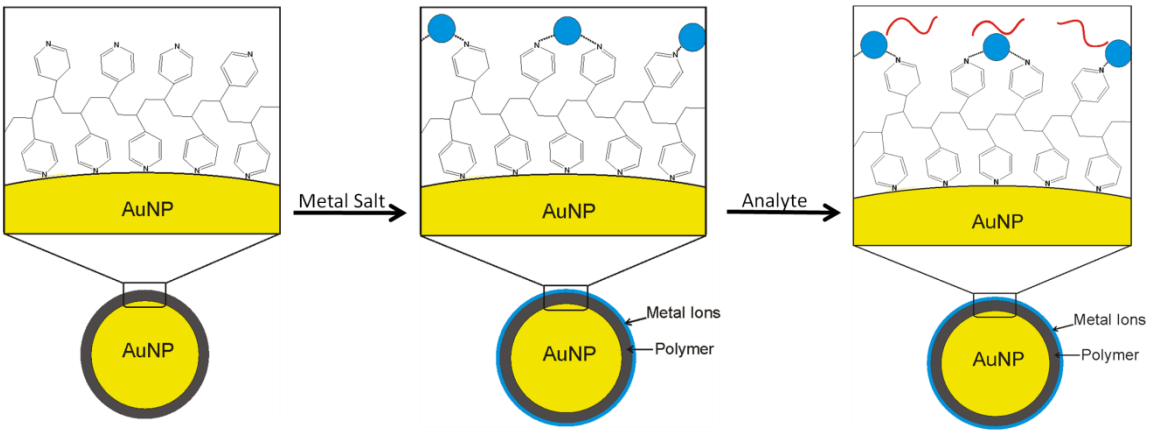

Scheme 4. A schematic representation of metal ion addition to the P4VP encapsulated AuNPs followed by the capture of specific analytes by coordination through the metal ions.

The synthesis of the P4VP/AuNPs is carried out using a method that leads to nanoparticles ideal for use in solution based enrichment techniques due to their stability and size (**Figure 17**) allowing simple clean up of samples following enrichment. Therefore, following the synthesis and metal ion coordination these MC/P4VP/AuNPs were applied to a specific PTM, oxidized cysteines in the form of cysteic acid. The ability for oxoacid PTM to coordinate with metal ions has been described previously in methods such as IMAC [110] and other metal ion based techniques [128,110]. To being testing the MC/P4VP/AuNPs ability to capture cysteic acid modified peptides two peptides were chosen containing one oxidation site apiece LVINVCoxLSQG and CoxLVINVLSQR. These peptides are very similar in sequence the main difference is the position of the cysteic acid.

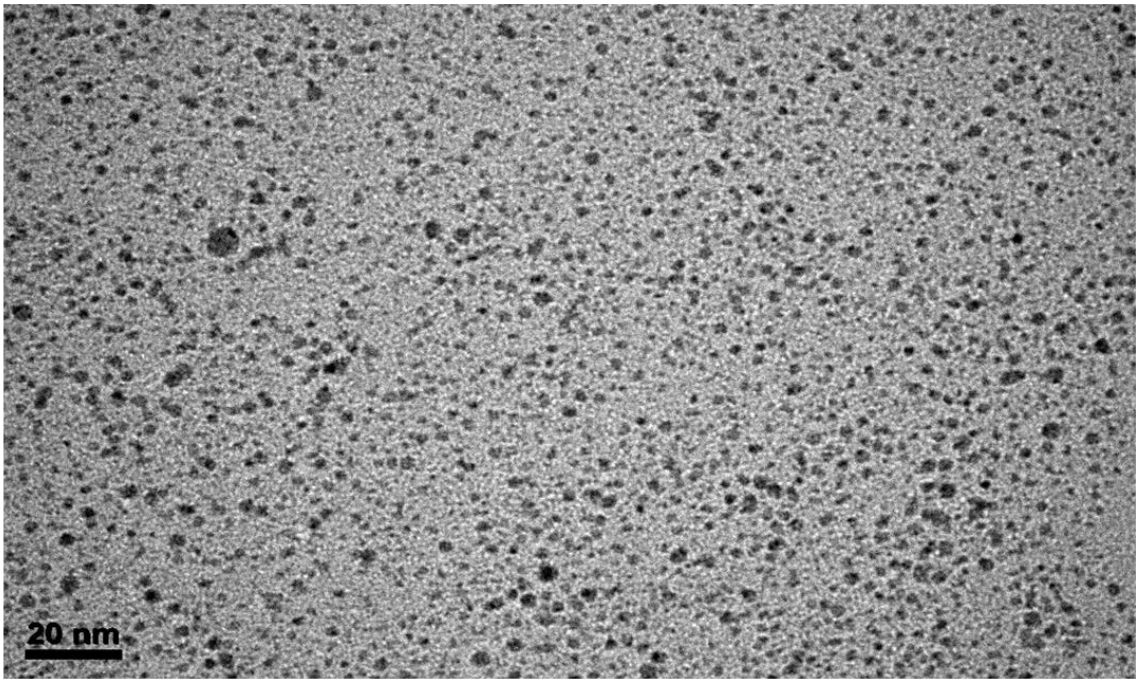

Figure 17. TEM image at 100k magnification of P4VP/AuNPs following synthesis and clean up. The scale bar is 20 nm.

The results of the enrichment of these to peptides at 100 µM using Fe^{3+}/ P4VP/AuNPs from water can been seen in **Figure 18**. The ability of Fe^{3+} ions to interaction with sulfonic acid has been studied previously for applications in heavy metal removal from water (refs). The enrichment of cysteic acid modified peptides using Fe^{3+} ions is similar to the enrichment of phosphorylated peptides using Fe^{3+} ions due to their structural and chemical characteristics being similar. The similarities in phospho and cysteic acid PTM allows for the use of the same metal ions; however, in proteomic research the ability to selectively enrich PTMs is necessary.

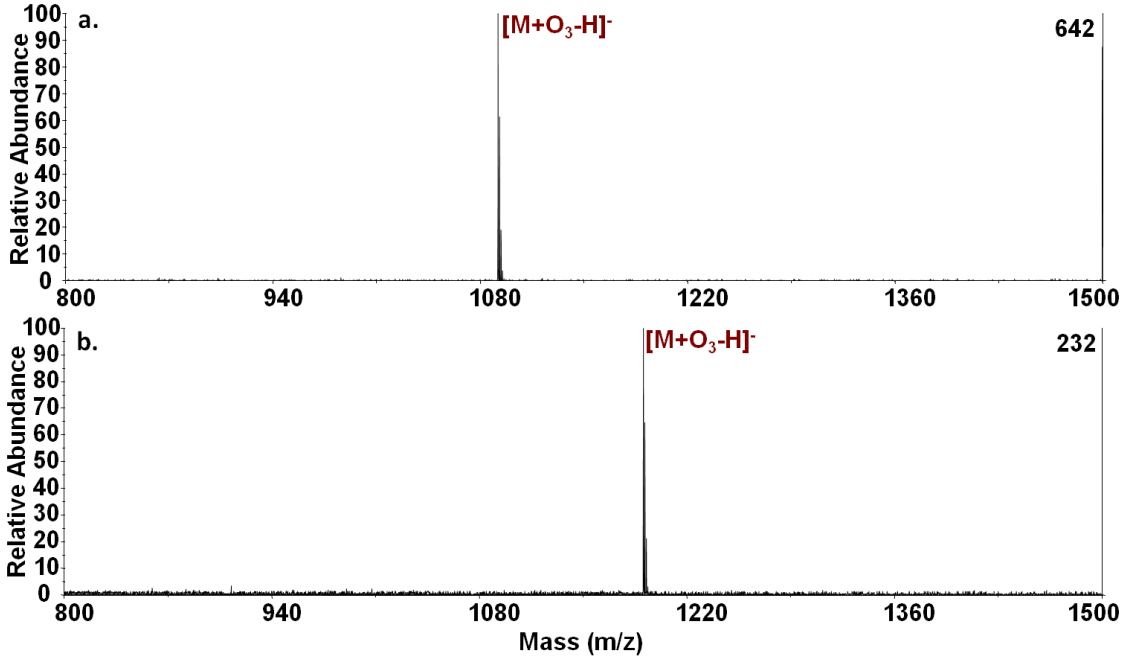

Figure 18. a. MALDI mass spectrum of 100 µM LVINVCoxLSQG after being captured using Fe^{3+}/P4VP/AuNPs. b. MALDI mass spectrum of 100 µM CoxLVINVLSQGR after being captured using Fe^{3+}/P4VP/AuNPs.

Due to the need for selectivity we changed the metal ions from Fe^{3+} to Mn^{2+}. Mn^{2+} was selected because other metal ions demonstrated to interact with R-SO_3H (ref) were tested for coordination to the P4VP/AuNPs. The other metal ions tested for coordination to the P4VP/AuNPs resulted in the aggregation of the AuNPs presumably because the P4VP polymer protecting the surface of the AuNPs was removed. This removal of the polymer from the surface of the AuNPs is due to the binding strength of the metal ions to the polymer being greater than the binding strength of the polymer to the surface of the AuNPs. These results led to Mn^{2+} being chosen as the metal ion used in place of Fe^{3+} for cysteic acid modified peptide enrichment using MC/P4VP/AuNPs. The first proof-of-

concept experiment wherein Mn^{2+}/P4VP/AuNPs were used to enrich cysteic acid modified peptide was performed using LVINVCoxLSQG at 100 µM where following the enrichment three wash steps using 18 MΩ H_2O, the results of the experiment are displayed in **Figure 19**. This result suggests the nature of the enrichment using Mn^{2+}/P4VP/AuNPs is based on a strong interaction between the Mn^{2+} ions and the R-SO_3H it is also similar to enrichment using Fe^{3+}/P4VP/AuNPs. Due to the results of this proof of concept experiment controls to ensure Mn^{2+}/P4VP/AuNPs enrich cysteic acid modified peptides is due to interaction of the Mn^{2+} were performed. The controls were tested using the unoxidized peptide LVINVCLSQG. The controls provide further evidence that the oxidized cysteine plays an important role in the enrichment because no signal for the LVINVCLSQG peptide was detected when using Mn^{2+}/P4VP/AuNPs mixed for enrichment.

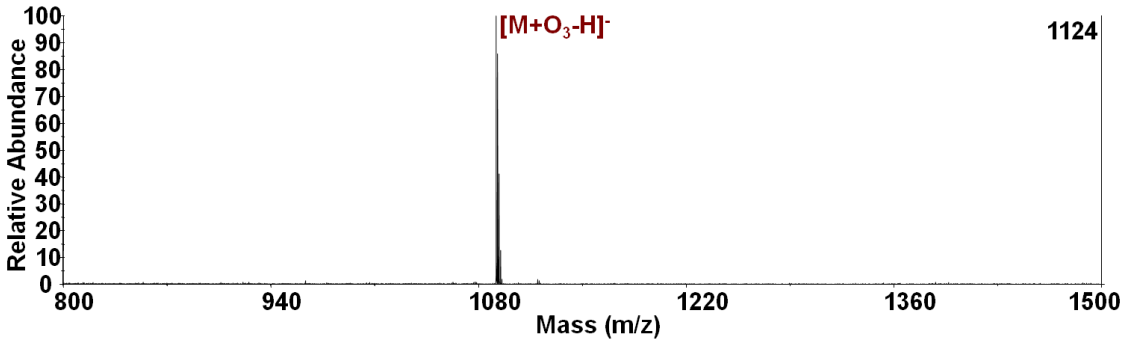

Figure 19. MALDI mass spectrum of 100 µM LVINVCoxLSQ after being captured using Mn^{2+}/P4VP/AuNPs.

To further test the ability of Mn^{2+}/P4VP/AuNPs to enrich cysteic acid modified peptides a mixture of LVINVCoxLSQG and human ACTH clip 18-39 in a 1:1 ratio was subjected to enrichment using Mn^{2+}/P4VP/AuNPs (see methods section). The results for this experiment are presented in **Figure 20**. These results are presented in both positive and negative ion mode because LVINVCoxLSQG produces predominantly negative ions unless alkali metal adducts are formed and the human ACTH clip 18-39 produces predominantly positive ions. This experiment demonstrates the ability of the MC/P4VP/AuNPs to enrich cysteic acid modified peptides even in the presence of acidic peptides. Acidic peptide binding to MC/P4VP/AuNPs has been previously described [88] also the binding of acidic peptides to metal ion affinity enrichment methods (IMAC) is also a known result. The ability of Mn^{2+}/P4VP/AuNPs to enrich cysteic acid modified peptides has been demonstrated but the selectivity of the method still needs to be explored.

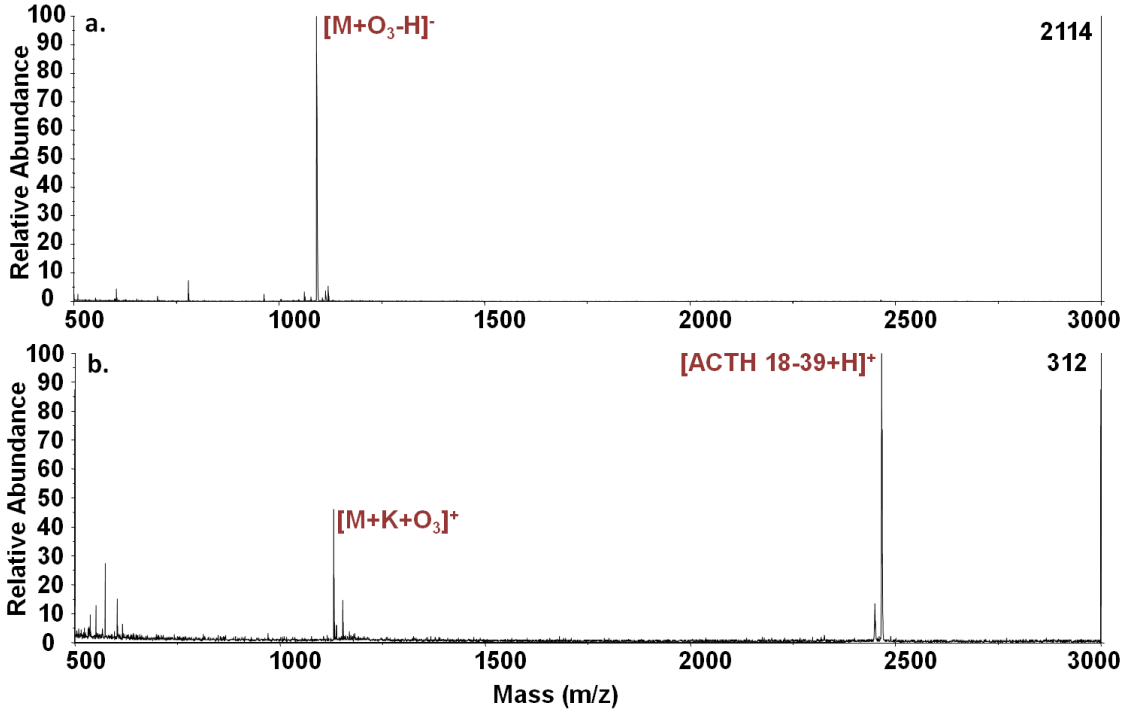

Figure 20. a. A negative mode MALDI mass spectrum using CHCA of a mix containing 100 µM LVINVCoxLSQG and 100 µM of human ACTH clip 18-39 after being captured using Mn^{2+}/P4VP/AuNPs. b. A positive mode MALDI mass spectrum using CHCA of a mix containing 100 µM LVINVCoxLSQG and 100 µM of human ACTH clip 18-39 after being captured using Mn^{2+}/P4VP/AuNPs.

To better characterize the selectivity of the Mn^{2+}/P4VP/AuNPs to enrich cysteic acid modified peptides over other similar PTMs such as phosphorylated peptides, experiments wherein both types of PTM modified peptides were present were performed. The four peptide mixture described in the material methods section containing two cysteic acid and two phosphopeptides was mixed with Mn^{2+}/P4VP/AuNPs. Following the enrichment method (see materials methods) the solution was analyzed using MALDI-MS CHCA (**Figure 21a, 21b**) and DHB (**Figure 22**). When analyzing the peptide mixture with CHCA before enrichment the ionization of the phosphopeptides is suppressed compared

to the ionization of the two cysteic acid peptides, **Figure 21a**. The preferential ionization of the cysteic acid peptides in the original mixture suggests that following enrichment the only peptides observed will be the cysteic acid peptides, this result is seen in **Figure 21b**. To better understand the enrichment selectivity of this method using the mixture of phosphopeptides and cysteic acid peptides a MALDI matrix needs to be selected that allows for the ionization of both types of peptides in the mixture.

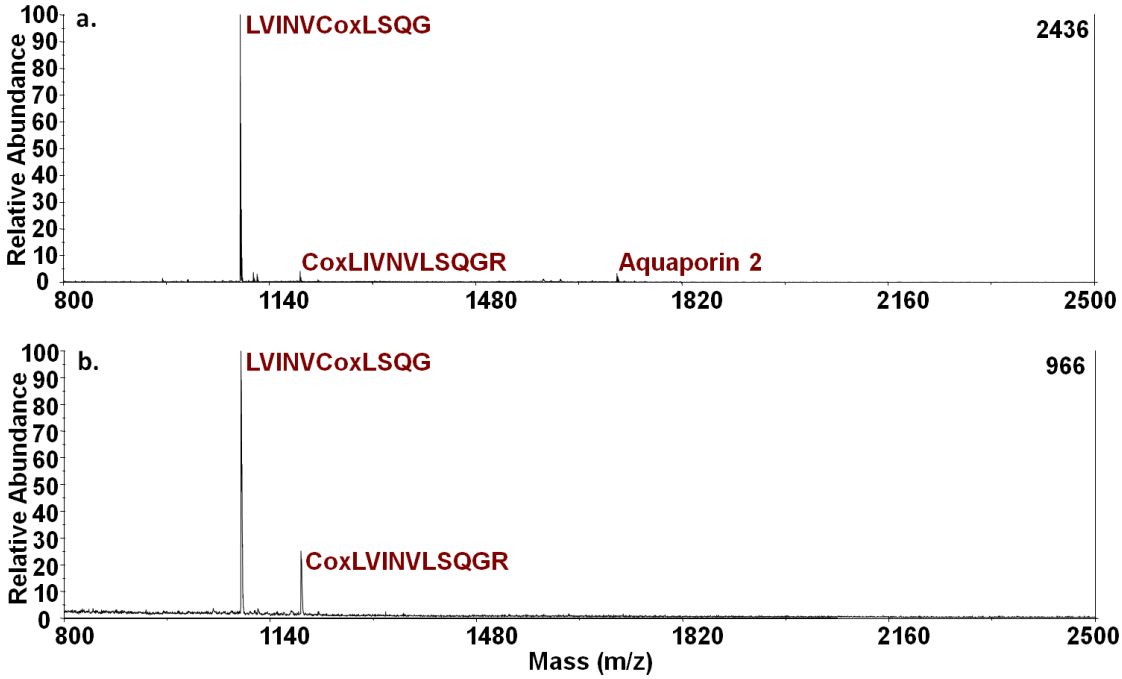

Figure 21. a. A negative mode MALDI mass spectrum using CHCA of a mix containing LVINVCoxLSQG, CoxLVINVLSQGR, Aquporin 2 and pp60 (v-src) each at 100 µM. b. A negative mode MALDI mass spectrum using CHCA of a mix containing LVINVCoxLSQG, CoxLVINVLSQGR, Aquaporin 2 and pp60 (v-src), each at 100 µM following enrichment Mn^{2+}/P4VP/AuNPs.

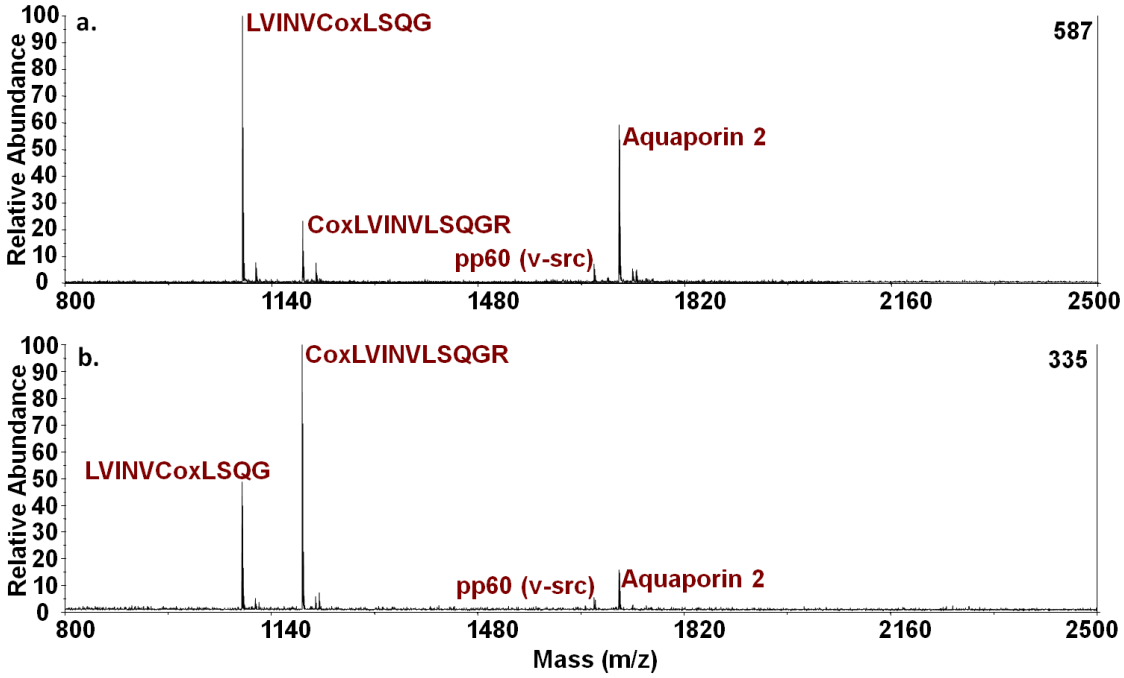

Figure 22. a. A negative mode MALDI mass spectrum using DHB of a mix containing LVINCoxLSQG, CoxLVINVLSQGR, Aquaporin 2 and pp60 (v-src) each at 100 µM. b. A negative mode MALDI mass spectrum using DHB of a mix containing LVINCoxLSQG, CoxLVINVLSQGR, Aquaporin 2 and pp60 (v-src) each at 100 µM following enrichment using Mn^{2+}/P4VP/AuNPs.

For this reason DHB was selected as the matrix of choice because it has been previously demonstrated to ionize phosphopeptides efficiently due to it being a relatively cool UV ionization matrix, thus allowing for the retention of labile posttranslational side chain modifications [129]. MALDI-MS analysis of the peptide mixture before enrichment using DHB as the matrix can be seen in **Figure 22a**. This result suggest that DHB will provide more insight into whether or not Mn^{2+} ions allow for selective enrichment of cysteic acid peptides over phospho peptides. The mass spectrum take from the peptide mixture following enrichment using Mn^{2+}/P4VP/AuNPs, **Figure 22b**, shows all four peptides

present in the mixture following enrichment using Mn^{2+} ions. The signals for the phosphopeptides in the mixture are not very abundant following the enrichment but they are still present suggesting the Mn^{2+} ions could be useful for enrichment of any oxoacid posttranslational modification. The results in **Figure 21** and **Figure 22** suggest the matrix chosen for use with this enrichment method plays an important role because the phosphopeptides are not well ionized with CHCA; however, when DHB is used as the matrix for the MALDI-MS experiment the phosphopeptides are ionized following enrichment using Mn^{2+}/P4VP/AuNPs. This data provides evidence that the use of metal ion coordination to selectively enrich oxoacid PTM (i.e. phosphorylation or cysteic acid) actually provides limited selectivity. However, once the PTMs have been enriched the ability to selectively ionize each PTM using different matrices has been demonstrated using CHCA for cysteic acid containing peptides and DHB for phosphorylation.

Conclusion

We have demonstrated the ability of MC/P4VP/AuNPs as a method for enrichment of cysteic acid containing peptides, the metal ions use for this PTM enrichment method were Fe^{3+} and Mn^{2+}. Fe^{3+} is a commonly used for enrichment of phosphorylation; therefore, Mn^{2+} was used as the metal ions in the MC/P4VP/AuNP method as a way to impart selectivity over other oxoacid PTM such as phosphorylation. The use Mn^{2+} ions to enrich cysteic acid containing peptides have been demonstrated; however, the selectivity of Mn^{2+} for cysteic acid containing peptides over phosphorylation is not evident. The ability to enrich both oxoacid PTMs then ionize selectively using CHCA

and DHB has been demonstrated. The ability to enrich whole subsets of PTMs using enrichment nanoparticles then selectively ionize individual PTM types from the nanoparticles opens the potential for a new type of enrichment methods.

CHAPTER V

CONCLUSIONS

With the focus of modern research trending toward biochemical issues, it is important to understand how molecules interact with surfaces, such as those of AuNPs and their protecting agents; this includes optimizing methods to analyze these molecules/systems. The use of poly(4-vinylpyridine) (P4VP) to synthesize AuNPs yields not only a small size distribution of AuNPs but incorporates a proton source into the system for use in LDI-MS. From this study we have demonstrated that the use of organic solvents to dissolve the peptides can disrupt the hydrophobic interactions between the amino acid side chains and the polymer subunits. This causes the ionization efficiencies to be lowered as a result of the decreased interaction with the AuNPs. Also involved in the lowering of the ionization efficiencies is the low availability of protons in the P4VP/AuNPs which could be an effect of the proton affinity of pyridine, which can be overcome by the solvent being used having excess protons incorporated within them. Therefore, we can conclude that solvent effects on peptides interactions are important and proton availability is also very important to consider when using P4VP/AuNPs for LDI-MS of peptides.

The capture of phosphorylated peptides using poly (4-vinylpyridine) (P4VP) encapsulated AuNPs with metal ions bound to the surface is reported using mass spectrometry was also studied in this research. We first demonstrated that Fe^{3+}/P4VP/AuNPs were able to capture phosphorylated peptides by using a single

phospho-peptide in water. Although the capture is possible using the AuNPs, we had to use a traditional MALDI matrix, DHB, because there is no protonation source available on the AuNPs with the metal ions and phospho-peptide bound. Using the AuNPs as the phospho-peptide capture "beads" in solution means there are fewer sample handling steps when compared to traditional phosphopeptide capture techniques.

The use of these MC/P4VP/AuNPs to capture phospho-peptides from a protein digest was also accomplished using two traditional IMAC metal ions, Fe^{3+} and Zn^{2+}. The ability to capture phospho-peptides from a protein digest using two different metal ions demonstrates the robustness of this method and the applicability of these AuNPs in traditional phosphoproteomic studies in a bottom up approach. This method also proves useful as a tool for whole protein capture and digests which allows for more applications in phosphoproteomic studies as a top-down technique.

We have also demonstrated the ability of MC/P4VP/AuNPs as a method for enrichment of cysteic acid containing peptides. Mn^{2+} was used as the metal ions in the MC/P4VP/AuNP method as a way to impart selectivity over other oxoacid PTM such as phosphorylation. The use Mn^{2+} ions to enrich cysteic acid containing peptides have been demonstrated; however, the selectivity of Mn^{2+} for cysteic acid containing peptides over phosphorylation is not evident. The ability to enrich both oxoacid PTMs then ionize selectively using CHCA and DHB is demonstrated. The ability to enrich whole subsets of PTMs using enrichment nanoparticles then selectively ionize individual PTM types from the nanoparticles opens the potential for a new type of enrichment methods.

REFERENCES

1. Dempster, A. A new method of postive ray analysis *Phys. Rev.* **1918**, *11*, 316-325.

2. Munson, M. S. B.; Field, F. H. Chemical ionization mass spectrometry. I. General introduction. *Journal of the American Chemical Society* **1966**, *88*, 2621-2630.

3. Morris, H. R.; Panico, M.; Barber, M.; Bordoli, R. S.; Sedgwick, R. D.; Tyler, A. Fast atom bombardment: a new mass spectrometric method for peptide sequence analysis. *Biochemical and Biophysical Research Communications* **1981**, *101*, 623-631.

4. Yamashita, M.; Fenn, J. B. Electrospray ion source. Another variation on the free-jet theme. *The Journal of Physical Chemistry* **1984**, *88*, 4451-4459.

5. Karas, M.; Bachmann, D.; Hillenkamp, F. Influence of the wavelength in high-irradiance ultraviolet laser desorption mass spectrometry of organic molecules. *Analytical Chemistry* **1985**, *57*, 2935-2939.

6. Tanaka, K.; Waki, H.; Ido, Y.; Akita, S.; Yoshida, Y.; Yoshida, T.; Matsuo, T. Protein and polymer analyses up to m/z 100 000 by laser ionization time-of-flight mass spectrometry. *Rapid Communications in Mass Spectrometry* **1988**, *2*, 151-153.

7. Aebersold, R.; Mann, M. Mass spectrometry-based proteomics. *Nature* **2003**, *422*, 198-207.

8. Smith, R. D.; Loo, J. A.; Loo, R. R. O.; Busman, M.; Udseth, H. R. Principles and practice of electrospray ionization-mass spectrometry for large polypeptides and proteins. *Mass Spectrometry Reviews* **1991**, *10*, 359-452.

9. Chiang, C.-K.; Chiang, N.-C.; Lin, Z.-H.; Lan, G.-Y.; Lin, Y.-W.; Chang, H.-T. Nanomaterial-based surface-assisted laser desorption/ionization mass spectrometry of peptides and proteins. *Journal of the American Society for Mass Spectrometry* **2010**, *21*, 1204-1207.

10. Lin, Z.-A.; Zheng, J.-N.; Lin, F.; Zhang, L.; Cai, Z.; Chen, G.-N. Synthesis of magnetic nanoparticles with immobilized aminophenylboronic acid for selective capture of glycoproteins. *Journal of Materials Chemistry* **2011**, *21*, 518-524.

11. Chen, C.-T.; Chen, Y.-C. Fe3O4/TiO2 core/shell nanoparticles as affinity probes for the analysis of phosphopeptides using TiO2 surface-assisted laser desorption/ionization mass spectrometry. *Analytical Chemistry* **2005**, *77*, 5912-5919.

12. Sherrod, S. D.; Diaz, A. J.; Russell, W. K.; Cremer, P. S.; Russell, D. H. Silver nanoparticles as selective ionization probes for analysis of olefins by mass spectrometry. *Analytical Chemistry* **2008**, *80*, 6796-6799.

13. Castellana, E. T.; Gamez, R. C.; Russell, D. H. Label-free biosensing with lipid-functionalized gold nanorods. *Journal of the American Chemical Society* **2011**, *133*, 4182-4185.

14. McLean, J. A.; Stumpo, K. A.; Russell, D. H. Size-selected (2-10 nm) gold nanoparticles for matrix assisted laser desorption ionization of peptides. *Journal of the American Chemical Society* **2005**, *127*, 5304-5305.

15. Wen, X.; Dagan, S.; Wysocki, V. H. Small-molecule analysis with silicon-nanoparticle-assisted laser desorption/ionization mass spectrometry. *Analytical Chemistry* **2006**, *79*, 434-444.

16. Vanderpuije, B. N. Y.; Han, G.; Rotello, V. M.; Vachet, R. W. Mixed monolayer-protected gold nanoclusters as selective peptide extraction agents for MALDI-MS analysis. *Analytical Chemistry* **2006**, *78*, 5491-5496.

17. Lin, P.-C.; Tseng, M.-C.; Su, A.-K.; Chen, Y.-J.; Lin, C.-C. Functionalized magnetic nanoparticles for small-molecule isolation, identification, and quantification. *Analytical Chemistry* **2007**, *79*, 3401-3408.

18. Jana, N. R.; Gearheart, L.; Murphy, C. J. Evidence for seed-mediated nucleation in the chemical reduction of gold salts to gold nanoparticles. *Chemistry of Materials* **2001**, *13*, 2313-2322.

19. Brust, M.; Walker, M.; Bethell, D.; Schiffrin, D. J.; Whyman, R. Synthesis of thiol-derivatised gold nanoparticles in a two-phase liquid-liquid system. *Journal of the Chemical Society, Chemical Communications* **1994**, 801-802.

20. Castellana, E. T.; Gamez, R. C.; Gomez, M. E.; Russell, D. H. Longitudinal surface plasmon resonance based gold nanorod biosensors for mass spectrometry. *Langmuir* **2010**, *26*, 6066-6070.

21. Castellana, E. T.; Russell, D. H. Tailoring nanoparticle surface chemistry to enchance laser desportion ionization of peptides and proteins. *Nano Lett.* **2007**, *7*, 3023-3025.

22. Jain, P. K.; Huang, X.; El-Sayed, I. H.; El-Sayed, M. A. Noble metals on the nanoscale: optical and photothermal properties and some applications in imaging, sensing, biology, and medicine. *Accounts of Chemical Research* **2008**, *41*, 1578-1586.

23. Link, S.; Wang, Z. L.; El-Sayed, M. A. Alloy formation of gold-silver nanoparticles and the dependence of the plasmon absorption on their composition. *J Phys Chem B* **1999**, *103*, 3529-3533.

24. Wilkins, M. R.; Pasquali, C.; Appel, R. D.; Ou, K.; Golaz, O.; Sanchez, J.-C.; Yan, J. X.; Gooley, A. A.; Hughes, G.; Humphery-Smith, I.; Williams, K. L.; Hochstrasser, D. F. From proteins to proteomes: large scale protein identification by two-dimensional electrophoresis and amino acid analysis. *Nat Biotech* **1996**, *14*, 61-65.

25. Zhang, Y.; Fonslow, B. R.; Shan, B.; Baek, M.-C.; Yates, J. R. Protein analysis by shotgun/bottom-up proteomics. *Chemical Reviews* **2013**, *113*, 2343-2394.

26. Li, Q.-r.; Ning, Z.-b.; Tang, J.-s.; Nie, S.; Zeng, R. Effect of peptide-to-TiO2 beads ratio on phosphopeptide enrichment selectivity. *Journal of Proteome Research* **2009**, *8*, 5375-5381.

27. Adamczyk, M.; Gebler, J. C.; Wu, J. Selective analysis of phosphopeptides within a protein mixture by chemical modification, reversible biotinylation and mass spectrometry. *Rapid Communications in Mass Spectrometry* **2001**, *15*, 1481-1488.

28. Chang, Y.-C.; Huang, C.-N.; Lin, C.-H.; Chang, H.-C.; Wu, C.-C. Mapping protein cysteine sulfonic acid modifications with specific enrichment and mass spectrometry: An integrated approach to explore the cysteine oxidation. *Proteomics* **2010**, *10*, 2961-2971.

29. Chait, B. T. Mass spectrometry: bottom-up or top-down? *Science* **2006**, *314*, 65-66.

30. Yang, Z.; Hancock, W. S. Approach to the comprehensive analysis of glycoproteins isolated from human serum using a multi-lectin affinity column. *Journal of Chromatography A* **2004**, *1053*, 79-88.

31. Feng, S.; Pan, C.; Jiang, X.; Xu, S.; Zhou, H.; Ye, M.; Zou, H. Fe3+ immobilized metal affinity chromatography with silica monolithic capillary column for phosphoproteome analysis. *Proteomics* **2007**, *7*, 351-360.

32. Kinoshita, E.; Yamada, A.; Takeda, H.; Kinoshita-Kikuta, E.; Koike, T. Novel immobilized zinc(II) affinity chromatography for phosphopeptides and phosphorylated proteins. *J Sep Sci* **2005**, *28*, 155-162.

33. Graves, J. D.; Krebs, E. G. Protein phosphorylation and signal transduction. *Pharmacology & Therapeutics* **1999**, *82*, 111-121.

34. Weckwerth, W.; Willmitzer, L.; Fiehn, O. Comparative quantification and identification of phosphoproteins using stable isotope labeling and liquid chromatography/mass spectrometry. *Rapid Communications in Mass Spectrometry* **2000**, *14*, 1677-1681.

35. Zhou, H.; Watts, J. D.; Aebersold, R. A systematic approach to the analysis of protein phosphorylation. *Nat Biotech* **2001**, *19*, 375-378.

36. Tao, W. A.; Wollscheid, B.; O'Brien, R.; Eng, J. K.; Li, X.-j.; Bodenmiller, B.; Watts, J. D.; Hood, L.; Aebersold, R. Quantitative phosphoproteome analysis using a dendrimer conjugation chemistry and tandem mass spectrometry. *Nat Meth* **2005**, *2*, 591-598.

37. Thompson, A. J.; Hart, S. R.; Franz, C.; Barnouin, K.; Ridley, A.; Cramer, R. Characterization of protein phosphorylation by mass spectrometry using immobilized metal ion affinity chromatography with on-resin β-elimination and michael addition. *Analytical Chemistry* **2003**, *75*, 3232-3243.

38. Lai, A. C.-Y.; Tsai, C.-F.; Hsu, C.-C.; Sun, Y.-N.; Chen, Y.-J. Complementary Fe3+- and Ti4+-immobilized metal ion affinity chromatography for purification of acidic and basic phosphopeptides. *Rapid Communications in Mass Spectrometry* **2012**, *26*, 2186-2194.

39. Wang, S.-T.; Wang, M.-Y.; Su, X.; Yuan, B.-F.; Feng, Y.-Q. Facile preparation of SiO2/TiO2 composite monolithic capillary column and its application in enrichment of phosphopeptides. *Analytical Chemistry* **2012**, *84*, 7763-7770.

40. Lim, K. B.; Kassel, D. B. Phosphopeptides enrichment using on-line two-dimensional strong cation exchange followed by reversed-phase liquid chromatography/mass spectrometry. *Analytical Biochemistry* **2006**, *354*, 213-219.

41. Seeley, E. H.; Riggs, L. D.; Regnier, F. E. Reduction of non-specific binding in Ga(III) immobilized metal affinity chromatography for phosphopeptides by using endoproteinase glu-C as the digestive enzyme. *Journal of Chromatography B* **2005**, *817*, 81-88.

42. Dong, M.; Wu, M.; Wang, F.; Qin, H.; Han, G.; Dong, J.; Wu, R. a.; Ye, M.; Liu, Z.; Zou, H. Coupling strong anion-exchange monolithic capillary with MALDI-TOF MS for sensitive detection of phosphopeptides in protein digest. *Analytical Chemistry* **2010**, *82*, 2907-2915.

43. D'Autreaux, B.; Toledano, M. B. ROS as signalling molecules: mechanisms that generate specificity in ROS homeostasis. *Nat Rev Mol Cell Biol* **2007**, *8*, 813-824.

44. Rhee, S. G. H2O2, a necessary evil for cell signaling. *Science* **2006**, *312*, 1882-1883.

45. Terada, L. S. Specificity in reactive oxidant signaling: think globally, act locally. *The Journal of Cell Biology* **2006**, *174*, 615-623.

46. Lee, S.-R.; Kwon, K.-S.; Kim, S.-R.; Rhee, S. G. Reversible inactivation of protein-tyrosine phosphatase 1B in A431 cells stimulated with epidermal growth factor. *Journal of Biological Chemistry* **1998**, *273*, 15366-15372.

47. Friguet, B. Oxidized protein degradation and repair in ageing and oxidative stress. *FEBS Letters*, *580*, 2910-2916.

48. Seo, Y. H.; Carroll, K. S. Profiling protein thiol oxidation in tumor cells using sulfenic acid-specific antibodies. *Proceedings of the National Academy of Sciences* **2009**, *106*, 16163-16168.

49. Jensen, S. S.; Larsen, M. R. Evaluation of the impact of some experimental procedures on different phosphopeptide enrichment techniques. *Rapid Communications in Mass Spectrometry* **2007**, *21*, 3635-3645.

50. Xu, Y.; Cao, Q.; Svec, F.; Fréchet, J. M. J. Porous polymer monolithic column with surface-bound gold nanoparticles for the capture and separation of cysteine-containing peptides. *Analytical Chemistry* **2010**, *82*, 3352-3358.

51. Lin, P.-C.; Chou, P.-H.; Chen, S.-H.; Liao, H.-K.; Wang, K.-Y.; Chen, Y.-J.; Lin, C.-C. Ethylene glycol-protected magnetic nanoparticles for a multiplexed immunoassay in human plasma. *Small* **2006**, *2*, 485-489.

52. Li, Y.-C.; Lin, Y.-S.; Tsai, P.-J.; Chen, C.-T.; Chen, W.-Y.; Chen, Y.-C. Nitrilotriacetic acid-coated magnetic nanoparticles as affinity probes for enrichment of histidine-tagged proteins and phosphorylated peptides. *Analytical Chemistry* **2007**, *79*, 7519-7525.

53 Garcia, M. E.; Baker, L. A.; Crooks, R. M. Preparation and characterization of dendrimer−gold colloid nanocomposites. *Analytical Chemistry* **1999**, *71*, 256-258.

54. Kotal, A.; Mandal, T. K.; Walt, D. R. Synthesis of gold–poly(methyl methacrylate) core–shell nanoparticles by surface-confined atom transfer radical polymerization at elevated temperature. *Journal of Polymer Science Part A: Polymer Chemistry* **2005**, *43*, 3631-3642.

55. Shan, J.; Chen, J.; Nuopponen, M.; Tenhu, H. Two phase transitions of poly(N-isopropylacrylamide) brushes bound to gold nanoparticles. *Langmuir* **2004**, *20*, 4671-4676.

56. Mayer, A. B. R.; Mark, J. E. Transition metal nanoparticles protected by amphiphilic block copolymers as tailored catalyst systems. *Colloid Polym Sci* **1997**, *275*, 333-340.

57. Sohn, B. H.; Seo, B. H. Fabrication of the multilayered nanostructure of alternating polymers and gold nanoparticles with thin films of self-assembling diblock copolymers. *Chemistry of Materials* **2001**, *13*, 1752-1757.

58. Hu, J.; Qian, Y.; Wang, X.; Liu, T.; Liu, S. Drug-loaded and superparamagnetic iron oxide nanoparticle surface-embedded amphiphilic block copolymer micelles for integrated chemotherapeutic drug delivery and MR imaging. *Langmuir* **2012**, *28*, 2073-2082.

59. Braun, G. B.; Lee, S. J.; Laurence, T.; Fera, N.; Fabris, L.; Bazan, G. C.; Moskovits, M.; Reich, N. O. Generalized approach to SERS-active nanomaterials via controlled nanoparticle linking, polymer encapsulation, and small-molecule infusion. *The Journal of Physical Chemistry C* **2009**, *113*, 13622-13629.

60. Möller, M.; Spatz, J. P.; Roescher, A. Gold nanoparticles in micellar poly(styrene)-b-poly(ethylene oxide) films—size and interparticle distance control in monoparticulate films. *Advanced Materials* **1996**, *8*, 337-340.

61. Hao, E. C.; Lian, T. Q. Buildup of polymer/Au nanoparticle multilayer thin films based on hydrogen bonding. *Chemistry of Materials* **2000**, *12*, 3392-3396.

62. Zhao, M.; Sun, L.; Crooks, R. M. Preparation of Cu nanoclusters within dendrimer templates. *Journal of the American Chemical Society* **1998**, *120*, 4877-4878.

63. Witze, E. S.; Old, W. M.; Resing, K. A.; Ahn, N. G. Mapping protein post-translational modifications with mass spectrometry. *Nat Meth* **2007**, *4*, 798-806.

64. Larsen, M. R.; Trelle, M. B.; Thingholm, T. E.; Jensen, O. N. Analysis of posttranslational modifications of proteins by tandem mass spectrometry. *Biotechniques* **2006**, *40*, 790.

65. Chen, Y.; Vertes, A. Adjustable fragmentation in laser desorption/ionization from laser-induced silicon microcolumn arrays. *Analytical Chemistry* **2006**, *78*, 5835-5844.

66. Lee, K.-H.; Chiang, C.-K.; Lin, Z.-H.; Chang, H.-T. Determining enediol compounds in tea using surface-assisted laser desorption/ionization mass spectrometry with titanium dioxide nanoparticle matrices. *Rapid Communications in Mass Spectrometry* **2007**, *21*, 2023-2030.

67. Stumpo, K. A.; Russell, D. H. Anion effects on ionization efficiency using gold nanoparticles as matrices for LDI-MS. *Journal of Physical Chemistry C* **2009**, *113*, 1641-1647.

68. Castellana, E. T.; Russell, D. H. Tailoring nanoparticle surface chemistry to enhance laser desorption ionization of peptides and proteins. *Nano Lett.* **2007**, *7*, 3023-3025.

69. Yan, B.; Zhu, Z. J.; Miranda, O. R.; Chompoosor, A.; Rotello, V. M.; Vachet, R. W. Laser desorption/ionization mass spectrometry analysis of monolayer-protected gold nanoparticles. *Anal Bioanal Chem* **2010**, *396*, 1025-1035.

70. Zhu, Z. J.; Ghosh, P. S.; Miranda, O. R.; Vachet, R. W.; Rotello, V. M. Multiplexed screening of cellular uptake of gold nanoparticles using laser desorption/ionization mass spectrometry. *Journal of the American Chemical Society* **2008**, *130*, 14139-14143.

71. Zhu, Z. J.; Rotello, V. M.; Vachet, R. W. Engineered nanoparticle surfaces for improved mass spectrometric analyses. *Analyst* **2009**, *134*, 2183-2188.

72. Murray, R. W. Nanoelectrochemistry: metal nanoparticles, nanoelectrodes, and nanopores. *Chem Rev* **2008**, *108*, 2688-2720.

73. Zhao, W.; Gao, Y.; Kandadai, S. A.; Brook, M. A.; Li, Y. DNA Polymerization on gold nanoparticles through rolling circle amplification: towards novel scaffolds for three-dimensional periodic nanoassemblies. *Angewandte Chemie International Edition* **2006**, *45*, 2409-2413.

74. Mössmer, S.; Spatz, J. P.; Möller, M.; Aberle, T.; Schmidt, J.; Burchard, W. Solution behavior of poly(styrene)-block-poly(2-vinylpyridine) micelles containing gold nanoparticles. *Macromolecules* **2000**, *33*, 4791-4798.

75. Chiu, J. J.; Kim, B. J.; Kramer, E. J.; Pine, D. J. Control of nanoparticle location in block copolymers. *Journal of the American Chemical Society* **2005**, *127*, 5036-5037.

76. Li, D.; He, Q.; Cui, Y.; Li, J. Fabrication of pH-responsive nanocomposites of gold nanoparticles/poly(4-vinylpyridine). *Chemistry of Materials* **2007**, *19*, 412-417.

77. Li, D.; He, Q.; Cui, Y.; Wang, K.; Zhang, X.; Li, J. Thermosensitive copolymer networks modify gold nanoparticles for nanocomposite entrapment. *Chemistry – A European Journal* **2007**, *13*, 2224-2229.

78. Wang, J.; Jensen, U. B.; Jensen, G. V.; Shipovskov, S.; Balakrishnan, V. S.; Otzen, D.; Pedersen, J. S.; Besenbacher, F.; Sutherland, D. S. Soft interactions at nanoparticles alter protein function and conformation in a size dependent manner. *Nano Lett.* **2011**, *11*, 4985-4991.

79. Shemetov, A. A.; Nabiev, I.; Sukhanova, A. Molecular interaction of proteins and peptides with nanoparticles. *ACS Nano* **2012**, *6*, 4585-4602.

80. Deng, Z. J.; Liang, M.; Toth, I.; Monteiro, M. J.; Minchin, R. F. Molecular interaction of poly(acrylic acid) gold nanoparticles with human fibrinogen. *ACS Nano* **2012**, *6*, 8962-8969.

81. Lundqvist, M.; Stigler, J.; Elia, G.; Lynch, I.; Cedervall, T.; Dawson, K. A. Nanoparticle size and surface properties determine the protein corona with possible implications for biological impacts. *Proceedings of the National Academy of Sciences* **2008**, *105*, 14265-14270.

82. Rodgers, M. T.; Stanley, J. R.; Amunugama, R. Periodic trends in the binding of metal ions to pyridine studied by threshold collision-induced dissociation and density functional theory. *Journal of the American Chemical Society* **2000**, *122*, 10969-10978.

83. Cammers-Goodwin, A.; Allen, T. J.; Oslick, S. L.; McClure, K. F.; Lee, J. H.; Kemp, D. S. Mechanism of stabilization of helical conformations of polypeptides by water containing trifluoroethanol. *Journal of the American Chemical Society* **1996**, *118*, 3082-3090.

84. Chatterjee, C.; Martinez, D.; Gerig, J. T. Interactions of trifluoroethanol with [val5]angiotensin II. *The Journal of Physical Chemistry B* **2007**, *111*, 9355-9362.

85. Buck, M. Trifluoroethanol and colleagues: cosolvents come of age. Recent studies with peptides and proteins. *Quarterly Reviews of Biophysics* **1998**, *31*, 297-355.

86. Zhou, H.; Tian, R.; Ye, M.; Xu, S.; Feng, S.; Pan, C.; Jiang, X.; Li, X.; Zou, H. Highly specific enrichment of phosphopeptides by zirconium dioxide nanoparticles for phosphoproteome analysis. *Electrophoresis* **2007**, *28*, 2201-2215.

87. Giron, P.; Dayon, L.; Mihala, N.; Sanchez, J.-C.; Rose, K. Cysteine-reactive covalent capture tags for enrichment of cysteine-containing peptides. *Rapid Communications in Mass Spectrometry* **2009**, *23*, 3377-3386.

88. Gaberc-Porekar, V.; Menart, V. Perspectives of immobilized-metal affinity chromatography. *Journal of Biochemical and Biophysical Methods* **2001**, *49*, 335-360.

89. Zhu, Z.-J.; Rotello, V. M.; Vachet, R. W. Engineered nanoparticle surfaces for improved mass spectrometric analyses. *Analyst* **2009**, *134*, 2183-2188.

90. Wuelfing, W. P.; Gross, S. M.; Miles, D. T.; Murray, R. W. Nanometer gold clusters protected by surface-bound monolayers of thiolated poly(ethylene glycol) polymer electrolyte. *Journal of the American Chemical Society* **1998**, *120*, 12696-12697.

91. Sun, W.; May, J. C.; Russell, D. H. A novel surface-induced dissociation instrument for ion mobility-time-of-flight mass spectrometry. *International Journal of Mass Spectrometry* **2006**, *in press.*

92. Stone, E. G.; Gillig, K. J.; Ruotolo, B. T.; Russell, D. H. Optimization of a matrix-assisted laser desorption ionization-ion mobility-surface-induced dissociation-orthogonal-time-of-flight mass spectrometer: simultaneous acquisition of multiple correlated MS1 and MS2 spectra. *International Journal of Mass Spectrometry* **2001**, *212*, 519-533.

93. Shipway, A. N.; Katz, E.; Willner, I. Nanoparticle arrays on surfaces for electronic, optical, and sensor applications. *Chemphyschem* **2000**, *1*, 18-52.

94. Shibamoto, K.; Sakata, K.; Nagoshi, K.; Korenaga, T. Laser desorption ionization mass spectrometry by using surface plasmon excitation on gold nanoparticle. *Journal of Physical Chemistry C* **2009**, *113*, 17774-17779.

95. Shen, J. W.; Ahmed, T.; Vogt, A.; Wang, J. Y.; Severin, J.; Smith, R.; Dorwin, S.; Johnson, R.; Harlan, J.; Holzman, T. Preparation and characterization of nitrilotriacetic-acid-terminated self-assembled monolayers on gold surfaces for matrix-assisted laser desorption ionization-time of flight-mass spectrometry analysis of proteins and peptides. *Analytical Biochemistry* **2005**, *345*, 258-269.

96. Shang, L.; Yin, J. Y.; Li, J.; Jin, L. H.; Dong, S. J. Gold nanoparticle-based near-infrared fluorescent detection of biological thiols in human plasma. *Biosensors & Bioelectronics* **2009**, *25*, 269-274.

97. Wilson, O. M.; Scott, R. W. J.; Garcia-Martinez, J. C.; Crooks, R. M. Synthesis, characterization, and structure-selective extraction of 1-3-nm diameter AuAg dendrimer-encapsulated bimetallic nanoparticles. *Journal of the American Chemical Society* **2005**, *127*, 1015-1024.

98. Wilson, O. M.; Scott, R. W. J.; Garcia-Martinez, J. C.; Crooks, R. M. Separation of dendrimer-encapsulated Au and Ag nanoparticles by selective extraction. *Chemistry of Materials* **2004**, *16*, 4202-4204.

99. Wijaya, A.; Schaffer, S. B.; Pallares, I. G.; Hamad-Schifferli, K. Selective release of multiple DNA oligonucleotides from gold nanorods. *ACS Nano* **2008**, *3*, 80-86.

100. Teng, C. H.; Ho, K. C.; Lin, Y. S.; Chen, Y. C. Gold nanoparticles as selective and concentrating probes for samples in MALDI MS analysis. *Analytical Chemistry* **2004**, *76*, 4337-4342.

101. Oh, S. K.; Niu, Y.; Crooks, R. M. Size-selective catalytic activity of Pd nanoparticles encapsulated within end-group functionalized dendrimers. *Langmuir* **2005**, *21*, 10209-10213.

102. Brust, M. F., J.; Bethell, D.; D. J. Schiffring, D.J.; and Kiely, C. Synthesis and reactions of functionalized gold nanoparticles. *J. Chem. Soc., Chem. Commun.,* **1995**, *16*, 1655-1656.

103. Sykora, C.; Hoffmann, R.; Hoffmann, P. Enrichment of multiphosphorylated peptides by immobilized metal affinity chromatography using Ga(III)- and Fe(III)-complexes. *Protein and Peptide Letters* **2007**, *14*, 489-496.

104. Corthals, G. L.; Aebersold, R.; Goodlett, D. R.: Identification of phosphorylation sites using microimmobilized metal affinity chromatography. *Methods in Enzymology*; Burlingame, A. L., Ed.; Academic Press, 2005; Vol. Volume 405; 66-81.

105. Sugiyama, N.; Masuda, T.; Shinoda, K.; Nakamura, A.; Tomita, M.; Ishihama, Y. Phosphopeptide enrichment by aliphatic hydroxy acid-modified metal oxide chromatography for nano-LC-MS/MS in proteomics applications. *Molecular & Cellular Proteomics* **2007**, *6*, 1103-1109.

106. Long, J. H.; Hull, M. On the optimum reaction in tryptic digestion. I. *Journal of the American Chemical Society* **1917**, *39*, 1051-1059.

107. Kinoshita, E.; Yamada, A.; Takeda, H.; Kinoshita-Kikuta, E.; Koike, T. Novel immobilized zinc(II) affinity chromatography for phosphopeptides and phosphorylated proteins. *J Sep Sci* **2005**, *28*, 155-162.

108. Andersson, L.; Porath, J. Isolation of phosphoproteins by immobilized metal (Fe3+) affinity chromatography. *Analytical Biochemistry* **1986**, *154*, 250-254.

109. Pan, C.; Ye, M.; Liu, Y.; Feng, S.; Jiang, X.; Han, G.; Zhu, J.; Zou, H. Enrichment of phosphopeptides by Fe3+-immobilized mesoporous nanoparticles of MCM-41 for MALDI and nano-LC–MS/MS analysis. *Journal of Proteome Research* **2006**, *5*, 3114-3124.

110. Dunn, J. D.; Reid, G. E.; Bruening, M. L. Techniques for phosphopeptide enrichment prior to analysis by mass spectrometry. *Mass Spectrometry Reviews* **2010**, *29*, 29-54.

111. Grimsrud, P. A.; Swaney, D. L.; Wenger, C. D.; Beauchene, N. A.; Coon, J. J. Phosphoproteomics for the masses. *ACS Chemical Biology* **2010**, *5*, 105-119.

112. Posewitz, M. C.; Tempst, P. Immobilized gallium(III) affinity chromatography of phosphopeptides. *Analytical Chemistry* **1999**, *71*, 2883-2892.

113. Voet, D., Voet, J. G.: Biochemistry 4ed., 2010.

114. Hu, W.; Tedesco, S.; McDonagh, B.; Sheehan, D. Shotgun redox proteomics in sub-proteomes trapped on functionalised beads: Identification of proteins targeted by oxidative stress. *Marine Environmental Research* **2010**, *69, Supplement 1*, S25-S27.

115. Leonard, S. E.; Reddie, K. G.; Carroll, K. S. Mining the thiol proteome for sulfenic acid modifications reveals new targets for oxidation in cells. *ACS Chemical Biology* **2009**, *4*, 783-799.

116. Kinumi, T.; Shimomae, Y.; Arakawa, R.; Tatsu, Y.; Shigeri, Y.; Yumoto, N.; Niki, E. Effective detection of peptides containing cysteine sulfonic acid using matrix-assisted laser desorption/ionization and laser desorption/ionization on porous silicon mass spectrometry. *Journal of Mass Spectrometry* **2006**, *41*, 103-112.

117. Prudent, M.; Girault, H. H. The role of copper in cysteine oxidation: study of intra- and inter-molecular reactions in mass spectrometry. *Metallomics* **2009**, *1*, 157-165.

118. Rabilloud, T.; Heller, M.; Gasnier, F.; Luche, S.; Rey, C.; Aebersold, R.; Benahmed, M.; Louisot, P.; Lunardi, J. Proteomics analysis of cellular response to oxidative stress: evidence for in vivo overoxidation of peroxiredoxins at their active site. *Journal of Biological Chemistry* **2002**, *277*, 19396-19401.

119. Lim, J. C.; Choi, H.-I.; Park, Y. S.; Nam, H. W.; Woo, H. A.; Kwon, K.-S.; Kim, Y. S.; Rhee, S. G.; Kim, K.; Chae, H. Z. Irreversible oxidation of the active-site cysteine of peroxiredoxin to cysteine sulfonic acid for enhanced molecular chaperone activity. *Journal of Biological Chemistry* **2008**, *283*, 28873-28880.

120. Sethuraman, M.; McComb, M. E.; Huang, H.; Huang, S.; Heibeck, T.; Costello, C. E.; Cohen, R. A. Isotope-coded affinity tag (ICAT) approach to redox proteomics: identification and quantitation of oxidant-sensitive cysteine thiols in complex protein mixtures. *Journal of Proteome Research* **2004**, *3*, 1228-1233.

121. Giron, P.; Dayon, L.; Sanchez, J.-C. Cysteine tagging for MS-based proteomics. *Mass Spectrometry Reviews* **2011**, *30*, 366-395.

122. Paulsen, C. E.; Carroll, K. S. Orchestrating redox signaling networks through regulatory cysteine switches. *ACS Chemical Biology* **2010**, *5*, 47-62.

123. Jacob, C.; Knight, I.; Winyard, P. G. Aspects of the biological redox chemistry of cysteine: from simple redox responses to sophisticated signalling pathways. *Biol Chem* **2006**, *387*, 1385-1397.

124. Danehy, J. P.; Elia, V. J. Determination of sulfinic acids in the presence of thiols by titration with aqueous sodium nitrite. *Analytical Chemistry* **1972**, *44*, 1281-1284.

125. Brittain, S. M.; Ficarro, S. B.; Brock, A.; Peters, E. C. Enrichment and analysis of peptide subsets using fluorous affinity tags and mass spectrometry. *Nat Biotech* **2005**, *23*, 463-468.

126. Wheeler, K. E.; Erickson, B. K.; Mueller, R.; Singer, S. W.; VerBerkmoes, N. C.; Hwang, M.; Thelen, M. P.; Hettich, R. L. Metal affinity enrichment increases the range and depth of proteome identification for extracellular microbial proteins. *Journal of Proteome Research* **2012**, *11*, 861-870.

127. Williams, B.; Barlow, C.; Kmiec, K.; Russell, W.; Russell, D. Negative ion fragmentation of cysteic acid containing peptides: cysteic acid as a fixed negative charge. *Journal of The American Society for Mass Spectrometry* **2011**, *22*, 1622-1630.

128. Wolschin, F.; Wienkoop, S.; Weckwerth, W. Enrichment of phosphorylated proteins and peptides from complex mixtures using metal oxide/hydroxide affinity chromatography (MOAC). *Proteomics* **2005**, *5*, 4389-4397.

129. Cramer, R.; Richter, W. J.; Stimson, E.; Burlingame, A. L. Analysis of phospho- and glycopolypeptides with infrared matrix-assisted laser desorption and ionization. *Analytical Chemistry* **1998**, *70*, 4939-4944.